Rotational Isomers in Stacked Macrocycles: Synthesis and Spectroscopic Properties of Peripherally Substituted (μ-Oxo)bis(phthalocyaninatosilicon) Compounds

Jörg Kleinwächter and Michael Hanack*

Contribution from the Institut für Organische Chemie der Universität Tübingen, Auf der Morgenstelle 18, D-72076 Tübingen, Germany

Received July 31, 1996[⊗]

Abstract: The synthesis and spectroscopic properties of a series of soluble octaalkoxy-substituted silicon phthalocyanine monomers, $(RO)_8PcSi(OSiMe_2tBu)L$, and μ-oxo-bridged dimers, $[(RO)_8PcSi(OSiMe_2tBu)]_2O$ (R = $H_{17}C_8$-, $H_{25}C_{12}$-, (±)-3,7-Me_2-C_8H_{15}-, (±)-2-Et-C_6H_{12}-; L = -$OSiMe_2tBu$, -$OSiMe_3$, -F, -OH), are reported. The optical absorption spectra of all dimers show strong solvatochromic behavior whereas the monomers do not. In nonaromatic solvents like, e.g., dichloromethane, the Q-band of the dimers is split into at least five broad bands between 560 and 760 nm, and proton NMR spectra show a strong splitting ($\Delta\delta$ = 1 ppm) of the aromatic signal at low temperature, indicating a torsion angle of ∼20−30° between the rings. In aromatic solvents such as, e.g., benzene, toluene, or 1-methylnaphthalene, thermochromism of the dimers is observed. This is shown by temperature-dependent optical absorption spectroscopy to be due to the presence of a second isomer exclusively found in solutions of aromatic solvents. It shows a rather different absorption spectrum with a very intense and sharp Q-band at 639 nm, a weak shoulder at ∼670 nm, and a very broad and weak absorption at ∼830 nm. Proton NMR spectra of this isomer show, even at −88 °C, only one signal for the aromatic protons, demonstrating a fully staggered or eclipsed conformation of the two rings. The ratio between the two isomers is dependent on the nature and concentration of the aromatic solvent molecules and the steric demand of the alkyl chains R attached to the macrocycle. The assignment of the absorption bands in both isomers is discussed in relation to exciton coupling theory and inter-ring $\pi-\pi$ interactions between the aromatic solvent and the macrocycles, which are likely to account also for the strong aromatic solvent-induced NMR shifts (ASIS) observed for the monomers as well as for the dimers.

Introduction

Polymeric, μ-oxo-bridged group IVA or μ-fluoro-bridged group IIIA phthalocyaninato metal-based materials $[PcMO]_n$ (M = Si, Ge, Sn)[1−4] or $[PcMF]_n$ (M = Al, Ga)[5,6] have attracted attention for more than 30 years, especially due to their electrical properties after doping.[7,8] These phthalocyaninato ring systems are forced into a coplanar face-to-face stacked arrangement by the bridging oxygen or fluorine atoms, with the stacking axis being perpendicular to the ring plane. This allows a unique way to investigate the influence of single parameters such as, e.g., the nature of the dopant or the intermolecular stacking distance, on the electronic structure of these materials.[9] The close interplanar distance between the macrocyclic π-systems (e.g., 3.30 Å in $[PcSiO]_nI_{1.1}$ and 3.48 Å in $[PcGeO]_nI_{1.1}$[4,10]) results in a strong $\pi-\pi$ overlap between adjacent molecular subunits. This causes the formation of a band structure composed entirely of ring π-orbitals which, after doping and thus creating a partly filled valence band, is responsible for the one-dimensional conductivity along the stacking axis. The -M−O−M- (M = Si, Ge, Sn) or -M−F−M- (M = Al, Ga) backbone is unlikely to play a direct role in the conduction process.[7,11] The bandwidth and, correlatively, the mobility of the charge carriers along the chain axis are mainly determined[9,12,13] by (i) the (fixed) interplanar distance and (ii) the torsion angle α between adjacent interacting macrocycles, which is probably influenced strongly by steric factors.[14] In $[PcSiO]_n$, this angle was found by X-ray powder diffraction techniques to be ∼39°,[4] whereas in less closely stacked systems, such as in $[PcGaF]_n$[6] or $[PcGeO]_n$,[4] eclipsed geometries are found. Furthermore, in peripherally substituted polymers $[R_mPcSiO]_n$ (R_m = e.g., $(tBu)_4$, $(H_{2n+1}C_nOCH_2)_8$, or $H_{2n+1}C_nO)_8$),[15−18] where the steric influence of the substituents might dominate the conformation, the torsion angle could well be considerably altered. The dependence of

* Corresponding author. Phone: int 49-7071/29-72432. Fax: int 49-7071/29-5244. E-mail: hanack@uni-tuebingen.de.

[⊗] Abstract published in *Advance ACS Abstracts,* October 15, 1997.

(1) Joyner, R. D.; Kenney, M. E. *Inorg. Chem.* **1962**, *1*, 717−718.
(2) Joyner, R. D.; Kenney, M. E. J. *Am. Chem. Soc.* **1960**, *82*, 5790−5796.
(3) Esposito, J. N.; Sutton, L. E.; Kenney, M. E. *Inorg. Chem.* **1967**, *6*, 1116−1120.
(4) Dirk, C. W.; Inabe, T.; Schoch, T. F., Jr.; Marks, T. J. *J. Am. Chem. Soc.* **1983**, *105*, 1539−1550.
(5) Linsky, J. P.; Paul, T. R.; Nohr, R. S.; Kenney, M. E. *Inorg. Chem.* **1980**, *19*, 3131−3135.
(6) Nohr, R. S.; Wynne, K. J. *J. Chem. Soc., Chem. Commun.* **1981**, 1210−1211.
(7) Schultz, H.; Lehmann, H.; Rein, M.; Hanack, M. *Structure and Bonding 74;* Springer: Heidelberg, 1991; p 41.
(8) Marks, T. J. *Science* **1985**, *227*, 881−889 and references therein.
(9) Whangbo, M.-H.; Stewart, K. R. *Isr. J. Chem.* **1983**, *23*, 133−138.
(10) Kroenke, W. J.; Sutton, L. E.; Joyner, R. D.; Kenney, M. E. *Inorg. Chem.* **1963**, *2*, 1064−1065.
(11) For a related class of polymers, -M−L−M-, where M = transition metal and L = bidendate conjugated ligand, such as, e.g., pyrazine, tetrazine, see: Hanack, M.; Lang, M. *Adv. Mater.* **1994**, *6*, 819. There is evidence that the conduction process in this class of compounds occurs along the -M−L−M- backbone rather than through the macrocycles.
(12) Canadell, E.; Alvarez, S. *Inorg. Chem.* **1984**, *23*, 573−579.
(13) Pietro, W. J.; Marks, T. J.; Ratner, M. A. *J. Am. Chem. Soc.* **1985**, *107*, 5387−5391.
(14) Anderson, A. B.; Gordon, T. L.; Kenney, M. E. *J. Am. Chem. Soc.* **1985**, *107*, 192−195.
(15) Metz, J.; Pawlowski, G.; Hanack, M. *Z. Naturforsch.* **1983**, *38B*, 378−382.
(16) (a) Sauer, T.; Wegner, G. *Mol. Cryst. Liq. Cryst.* **1988**, *162B*, 97−118. (b) Caseri, W.; Sauer, T.; Wegner, G. *Makromol. Chem., Rapid. Commun.* **1988**, *9*, 651−657.
(17) (a) Sirlin, C.; Bosio, L.; Simon, J. *J. Chem. Soc., Chem. Commun.* **1987**, 379−380; (b) **1988**, 236−237.
(18) van der Pol, J. F.; Zwicker, J. W.; Warmann, J. M.; de Haas, M. P. *Recl. Trav. Chim. Pays-Bas* **1990**, *109*, 208−215.

S0002-7863(96)02663-7 CCC: $14.00

the conduction bandwidth on the torsion angle is, therefore, of considerable interest and has been the target of several calculations.[9,12,13] The full understanding and control of α are, therefore, important prerequisites for a successful investigation and design of materials based on μ-oxo-bridged phthalocyaninato metal polymers.

μ-Oxo-bridged dimers $[R_nPcSiO]_2O$ (and their germanium analogues) can be considered as the simplest model compounds suitable to study the influence of substituents on the conformation and conformational effects on the $\pi-\pi$ interactions between adjacent macrocycles. The solid state structure for the peripheral unsubstituted dimer[19,20] has been reported and shows a torsion angle of 36.6° [21] (compared with 39° in the polymer). Calculations of the electronic structure have been carried out, demonstrating the strong dependence of the $\pi-\pi$ interaction[21−27] on the torsion angle α.[26,28,29] Little is known about the torsion angle α in solution and the UV spectra of the dimers remain, therefore, poorly understood.[14,27,29,30]

In this paper, we describe the synthesis and spectroscopic properties of a series of peripherally octaalkoxy-substituted (μ-oxo)bis(phthalocyaninatosilicon) compounds, $[(RO)_8PcSi(OSiMe_2tBu)]_2O$ (**10**) [RO = $H_{17}C_8O$ (**10a**), $H_{25}C_{12}O$ (**10b**), (±)-3,7-Me_2-$C_8H_{15}O$ (**10c**), (±)-2-Et-$C_6H_{12}O$ (**10d**)], and show how peripheral substituents can be used to control the torsion angle α on a rational basis. We demonstrate the influence of the torsion angle α on the electronic spectra in such compounds experimentally and attempt to obtain an understanding of the complicated UV spectra of the dimers.

Results and Discussion

Synthesis and Chemical Properties. Peripherally[31] unsubstituted μ-oxo-bridged bis-[(phthalocyaninato)silicon] compounds, $[PcSi(OSiR_3)]_2O$ ($OSiR_3$ = $OSi(n\text{-}C_6H_{13})_3$[22,23] $OSiMe_2tBu$,[20,24] $OSiMe(OSiMe_3)_2$,[30] $OSi(OSiMe_3)_3$),[32] have been prepared so far exclusively by thermal condensation of either a mixture of axially hydroxy- and chloro-substituted or pure hydroxy-substituted monomeric silicon phthalocyanines.

While our synthesis of the corresponding peripherally alkoxy-substituted μ-oxo-bridged dimers **10a**−**e** basically follows this route in so far as axially hydroxy-substituted monomers are reacted, quite a few modifications of the original procedure were necessary in order to obtain the pure dimers **10a**−**e** in reasonable yields. A new catalytic coupling reaction, applicable at room temperature, has been used rather than the usual thermal procedure for the condensation step (Scheme 1).

Dihydroxy(octaalkoxyphthalocyaninato)silicon compounds $(RO)_8PcSi(OH)_2$ (**5**) [(R = n-$H_{17}C_8$- (**5a**), $H_{25}C_{12}$- (**5b**), (±)-3,7-Me_2-C_8H_{15}- (**5c**), (±)-2-Et-C_6H_{12}- (**5d**)] were prepared by a procedure very similar to the one described in the literature[18] (Scheme 1) (see Experimental Section). Compounds **5**, substituted with (±)-3,7-Me_2-$C_8H_{15}O$ (**5c**) and (±)-2-Et-$C_6H_{12}O$ chains (**5d**) (and also all other compounds prepared from these materials) are expected to be mixtures of diastereomers since racemic instead of optically pure alkyl bromides were used for the preparation of the corresponding isoindolines **2c,d**.

Silylation of the dihydroxy(octaalkoxyphthalocyaninato)silicon compounds **5a**−**d** was done with $Me_2tBuSiOSO_2CF_3$ ($Me_2tBuOTf$) in dichloromethane solution in the presence of pyridine. $(RO)_8PcSi(OSiMe_2tBu)_2$ (**6a**−**d**) were obtained in quantitative yield within less than 1 h, even at temperatures below −40 °C. Silylation should be done at temperatures below 10 °C in order to avoid the formation of traces of dimers $[(RO_8)PcSi(OSiMe_2tBu)]_2O$ (**10a**−**d**). These new procedures were found to be more convenient and superior in yield than the conventional silylation procedure using chlorosilanes in refluxing pyridine.[33]

Treatment of the bissilylated monomer **6** with tetrabutylammonium fluoride and trifluoroacetic acid in dry tetrahydrofuran cleaves off selectively one of the two siloxy groups. The fluorine in **7** can then be displaced by a hydroxy group by reacting first with Me_3SiOTf in dichloromethane/pyridine at room temperature and subsequently quenching the reaction mixture with water. The byproduct $(RO)_8PcSi(OSiMe_2tBu)(OSiMe_3)$ (**9**) in the hydrolysis step can be separated easily by chromatography.

The condensation of the monomers turned out to be the crucial step in the synthesis of the dimers **10a**−**e**. Thermal condensation of the axial hydroxy-substituted monomers **5** (e.g., in refluxing pyridine) leads to mixtures containing at least 10−15% of oligomers higher than dimers. We were not able to separate the dimers from the higher oligomers by adsorption or gel permeation chromatography, neither before nor after silylation with $Me_2tBuSiOTf$ (not even in a semipreparative scale).

Attempts to prepare pure monomer−dimer mixtures by thermal condensation of monosiloxy-substituted monomers **8** failed. Despite the blocking of one side of the macrocycle, higher oligomers are formed.[5] Scrambling of the siloxy groups occurs and leads to the formation of higher oligomers.

We found that condensation of hydroxy-substituted monomers **5** or **8** can be achieved within hours at room temperature if pyridinium triflate (PyH^+OTf^-) is added as a coupling catalyst. Catalyzed condensation of the monosiloxy-substituted monomers **8** leads to monomers and dimers as almost the only products if the concentration of the catalyst is low enough and reaction times are kept short (see preparation of **10e** below). These nonpolar compounds can be separated from the reaction mixture easily by column chromatography.

Partial silylation of monomers **5** with 1 equiv of $tBuMe_2SiOTf$ at −30 °C (to prevent condensation in this initial step) leads to a mixture of monomers **5**, **6**, and **8** which oligomerize after the temperature is raised above +10 °C.

The mixed dimer **10e** was prepared by cross-coupling of monomers **5d** and **8a**. The bishydroxy-substituted monomer

(19) Schramm, C. S.; Scaringe, R. P.; Stojacovic, D. R.; Hofffman, B. J.; Ibers, J. A.; Marks, T. J. *J. Am. Chem. Soc.* **1980**, *102*, 6702−6713.
(20) Ciliberto, E.; Doris, K. A.; Pietro, P. J.; Reisner, G. M.; Ellis, D. E.; Fragala, I.; Herbstein, F. H.; Ratner, M. A.; Marks, T. J. *J. Am. Chem. Soc.* **1984**, *106*, 7748−7761.
(21) Crystal structure of the trimer $(Me_3SiO)_2MeSi\text{-}O\text{-}(PcSiO)_3\text{-}SiMe(OSiMe_3)_2$ reveals a staggering angle of 15.9° between adjacent macrocycles: Swift, D. R. Ph.D. Thesis, Case Western Reverse University, Cleveland, OH, 1970.
(22) Wheeler, B. L.; Nagasubramanian, G.; Bard, A. J.; Schechtman, L. A.; Dininny, D. R.; Kenney, E. *J. Am. Chem. Soc.* **1984**, *106*, 7404−7410.
(23) DeWulf, D. W.; Leland, J. K.; Wheeler, B. L.; Bard, A. J.; Batzel, D. A.; Dininny, D. R.; Kenney, M. E. *Inorg. Chem.* **1987**, *26*, 266−270.
(24) Mezza, T. M.; Armstrong, N. R.; Ritter, G. W.; Iafalice, J. P.; Kenney, M. E. *J. Electroanal. Chem.* **1982**, *137*, 227−237.
(25) Kane, A. R.; Sullivan, J. F.; Kenney, D. H.; Kenney, M. E. *Inorg. Chem.* **1970**, *9*, 1445−1448.
(26) Hush, N. S.; Woolsey, I. S. *Mol. Phys.* **1971**, *21*, 465−474.
(27) Hush, N. S.; Cheung, A. S. *Chem. Phys. Lett.* **1977**, *47*, 1−4.
(28) Pietro, W. J.; Ellis, D. E.; Marks, T. J.; Ratner, M. A. *Mol. Cryst. Liq. Cryst.* **1984**, *105*, 273−287.
(29) Ishikawa, N.; Ohno, O.; Kaizu, Y.; Kobayashi, H. *J. Phys. Chem.* **1992**, *96*, 8832−8839.
(30) (a) Janson, T. R.; Kane, A. R.; Sullivan, J. F.; Knox, K.; Kenney, M. E. *J. Am. Chem. Soc.* **1969**, *91*, 5210−5214. (b) Keppeler, U.; Kobel, W.; Siehl, H.-U.; Hanack, M. *Chem. Ber.* **1985**, *118*, 2095.
(31) In this paper, peripheral positions refer to the four vacant positions at each of the four benzene units of the phthalocyanine ring (1,2,3,4,8,9,-10,11,15,16,17,18,22,23,24,25-positions of the macrocycle, denoted as a and b in structure **1b**). However, in the following we deal only with peripheral substituents attached to the two outer sites of each benzene ring, the 2,3,9,10,16,17,23,24-positions of the macrocycle (a-positions in structure **1b**). Axial positions are meant to be the two axial coordination sites at the central hexacoordinated silicon atom.
(32) Esposito, J. N.; Lloyd, J. E.; Kenney, M. E. *Inorg. Chem.* **1966**, *5*, 1979−1984.
(33) For *N*,*O*-bis(trimethylsilyl)acetamide as silylating agent, see: Mooney, J. R.; Choy, C. K.; Knox, K.; Kenney, M. E. *J. Am. Chem. Soc.* **1975**, *97*, 3033−3038.

Scheme 1. Schematic Drawing of (a) the Corresponding Dimer $[PcSi(OSiR_3)]_2O$ (Side View and Top View, Demonstrating the Staggering Angle a)[a] and (b) The Silicon Phthalocyanines Used in This Work

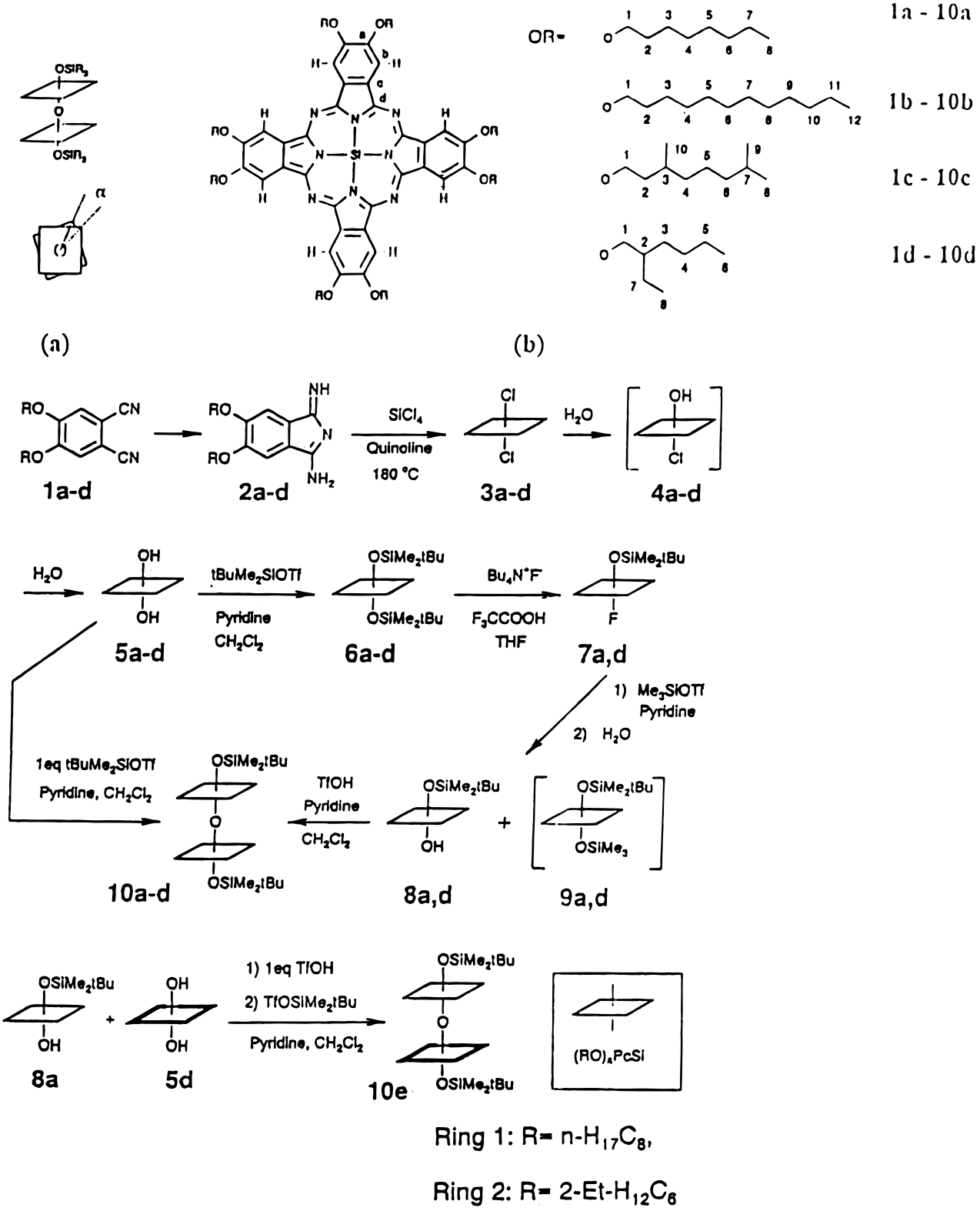

[a] The square represents a silicon phthalocyanine unit.

5d was chosen as the (2-ethylhexyl)oxy-substituted educt rather than **8d** in order to compensate somewhat for the low reactivity of this sterically hindered system.

Bissiloxy-substituted compounds **6** and **10** are all very soluble in common organic solvents. No aggregation of these compounds was ever observed. Hydroxy-substituted compounds **5**, on the other hand, are nearly insoluble in very polar (e.g., acetone, ethanol, DMF) or very unpolar (e.g., *n*-hexane) solvents but are still very soluble in aromatic or chlorinated hydrocarbons. Mainly aggregates are present in those solutions unless they are very diluted, as was shown by UV/visible and proton NMR spectroscopy.

The siloxy ligands in **6** and **8**−**10** (but not in **7**!) are sensitive to hydrolysis, especially under acidic conditions. The monomers are air stable in the solid state and stable for at least several days in solution as long as no acid is present, and chromatography on silica is possible without decomposition. The dimers are far less stable and should, therefore, be kept under nitrogen.

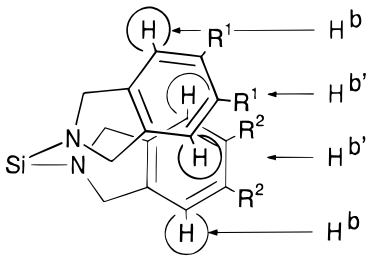

Figure 1. Schematic drawing of the top view of two isoindole units in the dimers [(RO)$_8$PcSi(OSiMe$_2$tBu)$_2$]O (**10**) for a torsion angle $\alpha \approx 22°$ (D_4 isomer). Note the position of H$^{b'}$, almost exactly above (or below) the center of the underlying (or overlying) benzene unit, causing a strong shielding[32] (see also Figure 7).

Proton NMR Spectra at Room Temperature. Proton NMR spectra of the axial bissiloxy-substituted monomers and dimers are generally well resolved in $CDCl_3$. In benzene-d_6 solvent, the signals of the axial siloxy ligands and of the aromatic protons H$^{b,b'}$ (see Figure 1) are as well resolved as in $CDCl_3$, but the signals of the middle parts of the alkyl chains are slightly broadened.

Proton NMR data for $CDCl_3$ and benzene-d_6 solutions of the octakis(*n*-octyloxy) substituted monomers and dimers **5a**−**10a** are shown in Table 1, together with the data for their precursor **1a**. All other compounds **5b**−**d** to **9b**−**d** show similar data (except for the aliphatic protons) as long as no aggregation takes place. Interaction between the macrocycles, resulting in the formation of aggregates, occurs mainly with the hydroxy-substituted species **5** and **8** and, to a minor extent, with the fluoro-substituted species **7**. Interacting monomers are marked with an asterisk in Table 1 and are discussed separately. For comparison, data of the peripherally unsubstituted compounds PcSi(OSiMe$_2$tBu)$_2$ and [PcSi(OSiMe$_2$tBu)]$_2$O, taken from ref 20, are included in Table 1.

The positions of the ^{1}H-NMR resonances of the monomers in $CDCl_3$ solution are clearly influenced by the strong ring current of the macrocycle and almost not affected by the peripheral alkoxy substitution. Protons in the axial positions of the macrocycle are strongly shielded and, therefore, shifted upfield, while the aromatic protons H$^{b,b'}$ (Figure 1), situated in the plane of the macrocycle, are shifted downfield. This is in accordance with earlier reports and with expectations.[30] Protons of the aliphatic chains are slightly but still significantly shifted to lower field, depending on their distance from the macrocycle, and appear, therefore, well separated from each other in the spectra.

In the dimers **10**, protons in the axial positions are further shifted upfield by the ring current of the second macrocycle, and chemical shifts of the aromatic protons are diminished, as has been found before.[30] As expected, all protons of the aliphatic chains are slightly more deshielded in the dimers than in the monomers, though this effect again decreases with increasing distance from the ring center.

Spectra taken in aromatic solvents differ significantly from those taken in CD_2Cl_2 or $CDCl_3$. In addition to the ring current effects, strong aromatic solvent-induced shifts (ASIS)[34,35] are observed. In benzene-d_6 solution, the protons of the axial ligands and the aromatic protons of the macrocycles in the monomer **6** as well as in the dimer **10** appear throughout deshielded by some 0.4−0.47 ppm relative to chloroform-d_6 solutions (see Table 1). Similar but far less pronounced effects are observed in the peripherally unsubstituted compounds,[20] e.g., the ASIS for the OSi-Me protons, the OSi-tBu protons, and the aromatic H$^{b,b'}$ protons are −0.28, −0.15, and −0.09, respectively, for PcSi(OSiMe$_2$tBu)$_2$. The same trend is observed for the dimers.[36] Solvent-induced shifts are observed also for the aliphatic chains in **6** and **10**, but they are opposite in sign.[37]

When the two sides of the macrocycle are substituted with different axial ligands as in **7**−**9** and the dimers **10**,[38] the CH_2 protons of the alkyl chains become diastereotopic. While this does not affect the spectra of the monomers significantly, in the dimers **10** the strong ring current of the second macrocycle causes a splitting of the CH_2 signals of the chains. This is most pronounced for the OCH_2 protons, being closest to the macrocycle (splitting $\Delta\delta = 0.1-0.3$ ppm in $CDCl_3$ and 0.4−0.6 ppm in benzene-d_6, see Table 1), but is still significant for protons attached to the next carbon (H^2) in **10a** and **10b** and is even clearly observed for the two diastereotopic methyl groups (H^{8,9}) in **10c**. Similar effects have been discussed previously in alkyl-substituted porphyrine[39] dimers. In compounds bearing chiral alkyl substituents, such as **7d**, **8d**, and **10c**−**e**, chains with *R*- and *S*-configuration become diastereomeric as a whole. This is reflected in further splitting of their proton NMR signals.

Monomers **6a**−**d** and **9a**−**d** and the dimers **10a**,**b** show sharp singlets (line width 1−2 Hz) for the aromatic protons H$^{b,b'}$, as is expected for nonaggregated compounds.[40] However, in the dimers **10c,d**,**e**, all substituted with alkoxy chains bearing a chiral center, the aromatic resonances are significantly broadened. This broadening is not caused by any kind of a dynamic process. The signal is split for the case of [(3,7-Me$_2$-C$_8$H$_{15}$O)$_8$-PcSi(OSiMe$_2$tBu)]$_2$O (**10c**) in CD_2Cl_2. In other solvents and for [(2-Et-C$_6$H$_{12}$O)$_8$PcSi(OSiMe$_2$tBu)]$_2$O (**10d**), the splitting is less pronounced and more difficult to observe. We explain these multiple splittings by the presence of diastereomers, which is confirmed by the observation that, in the unsymmetrical dimer **10e**, only one of the two siloxy signals for H^{Si-tBu} is split, while the other one remains as a sharp singlet with a line width of ∼1.4 Hz.

Optical Spectra of the Monomers. Optical spectra of monomers **3**−**9** are all very similar as long as no aggregation takes place. Numerical data for all compounds relevant to this paper are given in Table 2 for solutions in dichloromethane. The absorption maxima obtained for the nonaggregated monomers in benzene were found to be the same (±1 nm) as those found in dichloromethane solution.[41] All monomers show intense absorptions in the 700−600 and in the 400−300 nm regions. The same absorptions are found nearly unchanged in peripherally unsubstituted monomers and have been assigned as Q-band and B-band $\pi-\pi^*$ transitions of the macrocycle, respectively. The Q-band region is basically not affected by the peripheral alkoxy substitutions[42] (i.e., the HOMO and LUMO are almost equally affected by the alkoxy substitution). The broad transition at around 430 nm is typical for alkoxy-

(34) Defined as $\Delta\delta = \delta(CDCl_3) - \delta(C_6D_6)$.

(35) Engler, E. M.; Laszlo, P. *J. Am. Chem. Soc.* **1971**, *93*, 1317−1327.

(36) Note that chemical shifts in $CDCl_3$ are identical for **6a** and PcSi(OSiMe$_2$tBu)$_2$, as well as for **10a** and [PcSi(OSiMe$_2$tBu)]$_2$O (see Table 1).

(37) Chemical shifts are measured relative to the residual solvent signal. Since TMS itself experiences an aromatic solvent-induced upfield shift of 0.59 ppm compared to TMS as external standard (Jutila, M. *Acta Chem. Scand.* **1981**, *B35*, 503−506), the meanings of the size and, in particular, the sign of ASIS are not entirely clear.

(38) The second macrocycle is formally considered as an axial ligand in this case.

(39) See, e.g: (a) Collman, J. P.; Barnes, C. E.; Collins, T. J.; Brothers, P. J. *J. Am. Chem. Soc.* **1981**, *103*, 7030−7032. (b) Bushby, C. A.; Dolphin, D. *J. Magn. Reson.* **1976**, *23*, 211−220.

(40) Monomers **5a**−**d, 7a,d** (only in benzene-d_6), and **8a,d** show broadened H$^{b,b'}$ signals due to aggregation (see also Table 1).

(41) Molar absorption coefficients in benzene, however, differ significantly from those measured in dichloromethane solution, since half-widths are generally smaller in benzene solution. This is demonstrated in Table 2 for **6a** and **6d**. However, the product $\Delta H_w \epsilon$ remains constant when the solvent is changed, indicating the integrated molar absorption coefficient and, hence, the oscillator strength being unchanged (assuming a Gaussian shape).

Table 1. Proton NMR Data (at 27 °C, δ in ppm) for **1a** and **5a**−**10a**[a]

	$H^{b,b'}$ [b] (aromatic)	H^{1} (−OCH_2−)	H^{8} (−CH_3)	H^{Si-tBu} (axial ligands)	H^{Si-Me} (axial ligands)	alkyl protons (multiplets) (C^2−C^7)
			Chloroform-d_1 Solution			
5a*	8.4 vbr	4.3 br	0.95			2.0 (C^2, br); 1.5 (C^3, br); 1.55−1.25 (C^4−C^7, br)
6a	9.04	4.68	0.94	−1.45	−3.00	2.18 (C^2); 1.76 (C^3); 1.56 (C^4); 1.46 (C^5); 1.39 ($C^{6,7}$)
7a	9.03	4.67	0.94	−1.41	−2.95	2.18 (C^2); 1.77 (C^3); 1.57 (C^4); 1.46 (C^5); 1.40 ($C^{6,7}$)
8a*	8.7 br	4.5 br	0.95	−1.61 sl br	−3.19 sl br	2.11 (C^2, br); 1.70 (C^3, br); 1.65−1.30 (C^4−C7)
9a	9.03	4.68	0.94	−1.45	−3.00 [c]	2.18 (C^2); 1.76 (C^3); 1.56 (C^4); 1.46 (C^5); 1.38 ($C^{6,7}$)
10a	8.45[d]	4.82[e] (endo) 4.61 (exo)	1.01	−2.27	-4.03	2.33 (C^2); 1.92 (C^3); 1.69 (C^4); 1.59 (C^5); 1.49 ($C^{6,7}$)
1a	7.1	4.0	0.86			1.8 (C^2); 1.6−1.2 (C^3−C7)
$PcSi(OSiMe_2tBu)_2$	9.66[f1]			−1.43	−2.97	8.34 ($H^{a,a'}$)
$[PcSi(OSiMe_2tBu)]_2O$	9.00[f2]			−2.32	−4.08	8.30 ($H^{a,a'}$)
			Benzene-d_6 Solution			
5a*				very broad signals		
6a	9.48	4.14	0.97	−0.98	−2.32	1.88 (C^2); 1.55 (C^3); 1.35 (C^4−C^7)
7a*	8.88 br	3.79 br	1.01	−1.25	−2.60	1.86/1.81 ($C^{2,2'}$); 1.50−1.25 (C^3−C^7)
8a*	9.55 br	4.20 br	1.02	−1.36	−2.75	1.98 (C^2, br); 1.63 (C^3, br); 1.41 (C^4−C^7)
	9.13 br[g]	4.47 br[g]				
	6.74 br[f]	2.75 br[g]				
9a	9.44	4.14	0.96	−0.99	−2.34[c]	1.88 (C^2); 1.55 (C^3, br); 1.35 (C^4−C^7)
10a	9.11[h]	4.51 (endo) 4.05 (exo)	1.03	−1.84	−3.40	2.12 (C^2); 1.74 (C^3, br); 1.53 ($C^{4,5}$); 1.44 ($C^{6,7}$)
$PcSi(OSiMe_2tBu)_2$	9.75[e3]			−1.28	−2.69	7.87 ($H^{a,a'}$)
$[PcSi(OSiMe_2tBu)]_2O$	9.26[f4]			−2.16	−3.78	8.00 ($H^{a,a'}$)

[a] Asterisk indicates aggregates present. [b] Singlets, otherwise noted. [c] δ(-$OSiMe_3$) = −2.83 ($CDCl_3$) and −2.25 (C_6D_6). [d] In CD_2Cl_2, 8.49 ppm (27 °C); 8.9 ppm, 7.9 ppm (−88 °C, equal intensity). [e] Both signals are split at −88 °C in CD_2Cl_2. [f] To allow comparison with the values for the alkoxy-substituted systems, these shifts have to be corrected for two alkoxy substituents (in ortho and meta position): [e1]9.10; [e2]8.44; [e3]9.19; [e4]8.70 (Pretsch, E.; Clerc, T.; Seibl, J. *Tabellen zur Strukturaufklärung organischer Verbindungen mit spektroskopischen Methoden*, 1st edition; Springer-Verlag: New York, Heidelberg, Berlin, 1981; p H255). [g] Aggregate, see text. [h] 9.5 ppm at −88 °C (toluene-d_8).

Table 2. Optical Absorption Maxima (in nm) for Monomers $(RO)_8PcSiL_2$ in Dichloromethane Solutions at 25 °C[a]

	Q-band			CT band	Soret band (B-band)	
5a	680.1	651	612	430	358	340
5b	680.1	651	612	433	358	339
5c	680.3	651	612	432	358	340
5d	681.1	651	613	437	358	340
6a	675.6	645	609	427	357	338
$\epsilon(CH_2Cl_2)$		*(342, ΔH_w =30 nm)[b]*		*(28)*	*(139)*	*(74)*
$\epsilon(C_6H_6)$		*(437, ΔH_w = 23.5 nm)[b]*		*(31)*	*(160)*	*(78)*
6b	675.7	645	609	426	357	339
6c	676.1	646	609	427	357	338
6d	676.6	646	609	434	357	338
$\epsilon(CH_2Cl_2)$		*(354, ΔH_w =30 nm)[b]*		*(28)*	*(144)*	*(79)*
$\epsilon(C_6H_6)$		*(466, ΔH_w = 22.5 nm)[b]*		*(36)*	*(175)*	*(86)*
7a	680.6	650	613	430	352	~336
7d	681.6	651	614	437	352	~337
8a	678.1	648	610	429	358	339
8d	678.8	649	611	431	357	339
9a	675.5	645	608	426	357	338
9d	676.4	646	609	428	357	339

[a] Absorption maxima in benzene solution are almost identical. For compounds **6a** and **6d**, molar absorption coefficients and the half-width of the Q-band are given in italics. All compounds show additional transitions at 299 (±1 nm) and 280 nm (±2 nm). [b] Most intense Q-band transition ($Q_{0,0}$). $\Delta H_w \equiv$ full band width at half-height.

substituted phthalocyanines and has been assigned to an oxygen-to-ring n−π* CT transition.[43]

The data presented in Table 2 show that the electronic spectra of the monomers depend slightly but significantly on the nature of the axial ligands and are almost independent of the peripheral alkoxy substituents. If, e.g., the Q-band absorption maxima of the bissiloxy-substituted monomers **6** are considered as a reference value, the alteration of a siloxy ligand to OH, F, or Cl causes a significant red shift in the Q-band position of 2.2, 5.0, or 15.2 nm, respectively.

Optical Spectra of the Dimers. Electronic absorption spectra of the μ-oxo-bridged dimers **10** in different solvents are shown in Figures 2 and 3, while numerical data are compiled in Table 3. Figure 2a−c shows the electronic spectra of dimers **10a,c,d**, respectively, in dichloromethane (solid line) and benzene (dashed line) solution,[44] and Figure 3 shows the spectrum of **10a** (solid line) and **10d** (dashed line) in 1-methylnaphthalene (all at 25 °C). The spectrum changes dramatically when recorded in dichloromethane (Figure 2a, solid line). In this solvent, **10a** shows a multiple split Q-band with at least five transitions between 500 and 900 nm. Very similar spectra are obtained in other nonaromatic solvents like acetone, diethyl ether, tetrahydrofuran, $CDCl_3$, and *n*-hexane.[45] In benzene, the spectrum of **10a** (Figure 2a, dashed line) looks like a superimposition of those of **10a** in 1-methylnaphthalene (Figure 3, solid

(42) This is further confirmed by the finding that, in different positional isomers of tetrasubstituted alkoxyphthalocyanines, the Q-band remains nearly unchanged in position, and no splitting is observed, despite the lowered symmetry of the macrocycle. Hanack, M.; Schmid, G.; Sommerauer, M. *Angew. Chem., Int. Ed. Engl.* **1993**, *32*, 1422−1424. Sommerauer, M.; Rager, C.; Hanack, M. *J. Am. Chem. Soc.* **1996**, *118*, 10085−10093.

(43) Gasyna, Z.; Kobayashi, N.; Stillman, M. J. *J. Chem. Soc., Dalton Trans.* **1989**, 2397−2405.

(44) The spectra of **10b** shown in Figure 4 are very similar to those of **10a**.

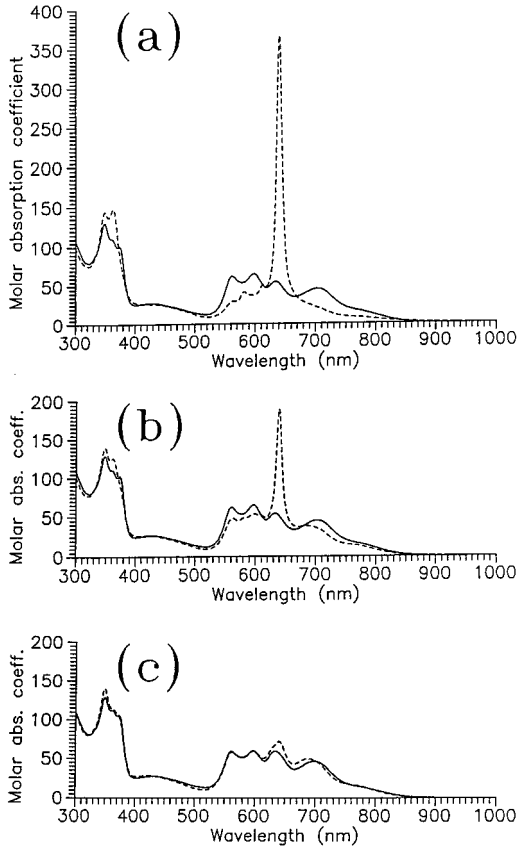

Figure 2. Electronic absorption spectra of (a) $[(H_{17}C_8O)_8PcSi(OSiMe_2tBu)_2]O$ (**10a**), (b) $[(3,7\text{-}Me_2\text{-}C_8H_{15}O)_8PcSi(OSiMe_2tBu)_2]O$ (**10c**), and (c) $[(2\text{-}Et\text{-}C_6H_{12}O)_8PcSi(OSiMe_2tBu)_2]O$ (**10d**) in benzene (dashed lines) and dichloromethane (solid lines) solution at 25 °C.

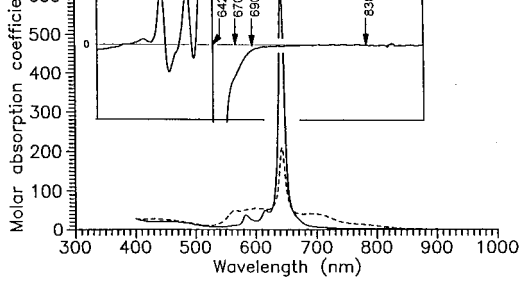

Figure 3. Electronic absorption spectra of $[(H_{17}C_8O)_8PcSi(OSiMe_2tBu)_2]O$ (**10a**) (solid line) and $[(2\text{-}Et\text{-}C_6H_{12}O)_8PcSi(OSiMe_2tBu)_2]O$ (**10d**) (dashed line) in 1-methylnaphthalene solution at 25 °C. Inset: First derivative of the spectrum of **10a**.

line) and **10a** in dichloromethane (Figure 2a, solid line).[20] Compounds **10b**−**e** all behave similarly to compound **10a** (see Figure 2b,c and Table 3).

The UV spectra of dimers **10a**−**d** were also measured in mixtures of dichloromethane and benzene. The result is shown for **10b** in Figure 4. For mixing ratios (mol %) between 100% benzene and 40% benzene− 60% dichloromethane, we observe (almost) isosbestic points, while the appearance of the spectrum changes dramatically. In the more polar mixtures ranging from 70% to 100% dichloromethane, the spectrum does not change much any longer. However, in the spectral range between 600 and 750 nm, there is a continuous shift and change in intensity of the transition around 700 nm, and, as a consequence the two isosbestic points between 600 and 700 nm blur out, while all the others remain sharp. We assign this shift to be a "normal" solvatochromic shift. The reason for the dramatic solvatochromy in the less polar solvent mixtures must be different. The change in intensity of the transitions, whereas their positions remain nearly unchanged, and the presence of isosbestic points cannot be explained in the same way. Bands do not shift at all, but new transitions gradually arise while others decrease. It therefore seems that two different isomers of the dimer, showing two different electronic absorption spectra, are present in a solvent-dependent equilibrium. To demonstrate this point, we measured the spectra of **10a**−**d** in toluene as a function of the temperature (25−80 °C and at −73 °C).[46] For **10a**−**c**, we find the spectra to be temperature dependent between 25 and 80 °C (see Figure 5 for **10b**), and we obtain isosbestic points.[47] Since the solvent does not change, they are sharp as expected, indicating the presence of two isomers of the dimeric phthalocyanine being in equilibrium.

It appears that, in dichloromethane solution (and in all other nonaromatic solvents we have tried), only one isomer is stable, irrespective of the temperature, the nature of the peripheral alkoxy substituents, and the axial ligands. The electronic spectrum of this blue isomer (Figure 2a−c, solid lines) shows the absence of any shoulder at 639 nm, proving the absence of the other isomer. In aromatic solvents (or mixtures of aromatic and nonaromatic solvents), mixtures of this blue isomer and a green one are present, the equilibrium being dependent on solvent (Figure 4), temperature (Figure 5), and peripheral substituents (Figure 2a−c, dashed lines, and Figure 3). The UV/vis spectrum of the green isomer is almost the same as the one shown in Figure 3 (solid line). However, a small amount of the blue isomer is still present in both cases, as indicated by the weak residual transitions at ∼700 nm.

The pure spectra of both isomers in toluene can be calculated according to eqs 1a and 1b by subtracting two spectra taken at different temperatures in toluene. The factors x (to obtain the

$$\epsilon(\lambda, \text{blue isomer}) = [\epsilon(\lambda,T_1) - x\epsilon(\lambda,T_2)]/(1-x) \quad T_1 > T_2 \tag{1a}$$

$$\epsilon(\lambda, \text{green isomer}) = [\epsilon(\lambda,T_2) - y\epsilon(\lambda,T_1)]/(1-y) \quad T_1 > T_2 \tag{1b}$$

spectrum of the blue isomer) and y (to obtain the spectrum of the green isomer) are chosen so that the transitions of the other isomer vanish, and no negative absorptions are obtained.

The spectra extrapolated by this procedure are shown in Figure 6, and numerical data are set out in Table 3 for **10a**. Spectra obtained for **10b** and **10c** are identical, and this demonstrates that the different diastereomers of **10c** do not show different electronic absorption spectra.

The thermodynamic parameters ΔH and ΔS are calculated from the temperature-dependent absorption spectra. For **10a** (in toluene), $\Delta H = 21$ kJ/mol and $\Delta S = 71$ J/(mol K) are obtained. As expected, slightly different values of $\Delta G(T)$ are found for **10c**, but the ln K versus l/T plot did not unequivocally reveal if this is caused by a different value for ΔS or for ΔH.

(45) Similar solvatochromic behavior was published recently for the dimer $((MeO)_4(H_{17}C_8O)_4PcSi(OH))_2O$. The reported absorption spectra of this compound are, however, blurred out by aggregation caused by the axial hydroxy ligands, traces of monomer (peak at 680 nm), and possibly the presence of positional isomers. Fernecz, A.; Neher, D.; Schulze, M.; Wegner, G.; Viane, L.; De Schryver, F. C. *Chem. Phys. Lett.* **1995**, *245*, 23−29.

(46) For **10d** also at −53, −33, −13, and +7 °C.

(47) Results for **10a** are very similar to those obtained for **10b**. For **10c**, the temperature dependence of the spectrum is somewhat less pronounced. Isobestic points in which three or even more species are in equilibrium are possible, see: Mayer, R. G.; Drago, R. S. *Inorg. Chem.* **1976**, *15*, 2010−2011. However, these special cases are not relevant to our results.

Table 3. Optical Absorption Data (in nm) for Compounds $[(RO)_8PcSi(OSiMe_2tBu)]_2O$ (**10**) in various solvents at 25 °C[a]

	Q-band						CT band	Soret band (B-band)			N-band	f[g]
					Dichloromethane, 25 °C							
10a	~760	703	634		598	561	429*br*	~373	~361	349	298	1.16[f]
	(sh)	*(45.2)*	*(54.4)*		*(64.6)*	*(61.7)*	*(27.4)*	*(100)*	*(sh)*	*(130)*	*(109)*	
10b	~760	702	634		598	561	428*br*	~373	~360	349	297	1.20
	(sh)	*(46.2)*	*(56.4)*		*(66.8)*	*(63.7)*	*(28.9)*	*(104)*	*(sh)*	*(135)*	*(119)*	
10c	~760	702	633		597	561	429*br*	373	~360	348	297	1.19
		(47.3)	*(56.3)*		*(67.3)*	*(64.5)*	*(27.6)*	*(106)*	*(115)*	*(134)*	*(115)*	
10d	~760	699	634		598	561	432*br*	372	361	349	297	1.17
	(sh)	*(46.9)*	*(50.0)*		*(60.2)*	*(59.5)*	*(27.4)*	*(106)*	*(113)*	*(129)*	*(113)*	
10e	~760*sh*	701	634		598	561	430*br*	373	~360*sh*	349	297	
					Benzene, 25 °C							
10a	~760	~687	639	613	596	581	565	424*br*		363	349	295	1.20
	(sh)	*(sh)*	*(366)*	*(50.4)*	*(37.4)*	*(41.7)*	*(29.7)*	*(26.2)*		*(148)*	*(144)*	*(105)*	
10b	~760	~687	639	613		581	565	426*br*		363	349	295	1.25
	(sh)	*(sh)*	*(369)*	*(53.1)*		*(44.2)*	*(32.6)*	*(27.4)*		*(150)*	*(152)*	*(110)*	
10c	~760	687	639	~612	598	583*sh*	562	424*br*	~372	362	348	296	1.21
		(39.0)	*(193.2)*	*(sh)*	*(54.7)*	*(49.8)*	*(49.0)*	*(26.9)*	*(sh)*	*(129)*	*(142)*	*(107)*	
10d	~760	687	640		598		563	423*br*	372*sh*	361sh	349	297	1.21
	(sh)	*(50.2)*	*(72.5)*		*(50.0)*		*(58.4)*	*(28.5)*	*(104)*	*(115)*	*(141)*	*(109)*	
10e	~760*sh*	687	639		597	~582sh	562	418*br*	~372*sh*	361*sh*	349	297	
					1-Methylnaphthalene, 25 °C							
10a	~826*br*	~700[d]	642	616	597	583	565	449*br*	solvent absorption				1.21
	(2.60)	*(sh)*	*(627)*	*(50.6)*	*(sh)*	*(38.0)*	*(sh)*	*(21.4)*					
10d		691	643	614	600	~587	566	434*br*					1.26
		(42.1)	*(212)*	*(54.9)*	*(56.0)*	*(sh)*	*(50.5)*	*(27.6)*					
					Toluene							
10a[b]	~760	~687	639	612		581	564	424 *br*		363	350		1.18
	(sh)	*(sh)*	*(360)*	*(50.3)*		*(43.8)*	*(32.5)*	*(23.6)*		*(150)*	*(139)*		
green	~836		639	612		580	562	455 *br*		363	350		
D_{4d}[c]	*(5.2)*		*(750)*	*(53.5)*		*(40.7)*	*(10.7)*	*(28.4)*		*(215)*	*(sh)*		
blue	~755	686	~636		598		564	~415sh	~370		348		
D_4[c]	*(sh)*	*(45.3)*	*d*		*(57.9)*		*(53.8)*	*(25.0)*	*(sh)*		*(131)*		

[a] Molar absorption coefficients ϵ (in 10^3L/(mol cm)) are given in parentheses. [b] At 25 °C. [c] Extrapolated data for the pure isomer, see text. [d] No reliable data available, see text. [e] 670 nm, sh. [f] 0.79 for monomer **6a** in CH_2Cl_2. [g] Oscillator strength of the Q-band (520−1000 nm). [g] 4.32×10^{-9} ($\int \epsilon \, d\upsilon$).

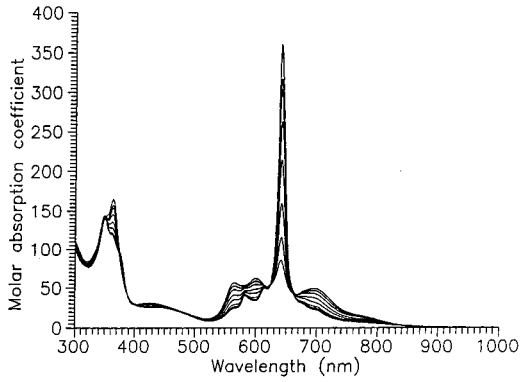

Figure 4. Electronic absorption spectra of $[(H_{25}C_{12}O)_8PcSi(OSiMe_2tBu)_2]O$ (**10b**) in different solvent mixtures benzene−dichloromethane at 25 °C. Solvent compositions are given in mol % benzene, in decreasing order of the molar absorption coefficient at 639 nm: 100%, 95%, 90%, 80%, 70%, 60%, 50%, and 40%.

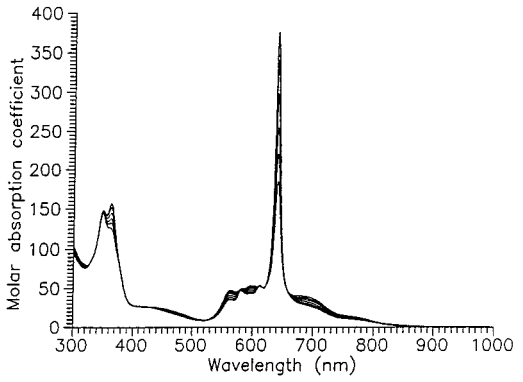

Figure 5. Electronic absorption spectra of $[(H_{25}C_{12}O)_8PcSi(OSiMe_2tBu)_2]O$ (**10b**) in toluene at different temperatures. Temperatures are given in decreasing order of the molar absorption coefficient at 639 nm: 26.2, 33.9, 42.0, 51, 60.3, and 70.7 °C.

In the μ-oxo-bridged dimers, the close stacking of the two macrocycles caused the two π-systems to interact. Modifications of the Q-band, consequently, are likely to be due to some change in the relative orientation of the rings. It seems reasonable to assign the blue isomer with the multipeaked Q-band (Figure 6, upper spectrum) as the less symmetrical one and the green one with the "normal", single Q-band (Figure 6, lower spectrum) as the more symmetrical one. The rotation of one macrocycle with respect to the other by an angle α around the central Si−O−Si bond produces conformations of D_{4h} ($\alpha = 0°$), D_4 ($0° < \alpha < 45°$), and D_{4d} ($\alpha = 45°$) symmetry, respectively (see Figure 7). The multipeaked spectra can be attributed to the symmetry D_4 and the one with a single Q-band to the symmetry D_{4h} or—for steric reasons—more probably D_{4d} (see discussion).

Proton NMR Spectra at Low Temperature. Confirmation for this interpretation comes from low-temperature ^{1}H-NMR studies of **10a**−**d**. As described before, the room temperature ^{1}H-NMR spectra of these compounds show in dichloromethane as well as in toluene one (**10a** and **b**) or several closely spaced (**10c**, **d**, or **e**) singlets for the aromatic protons $H^{b,b'}$ (Figure 1). However, the $H^{b,b'}$ protons are equivalent only under D_{4d} or D_{4h} symmetry, but not under D_4 symmetry, as demonstrated in Figure 1. Therefore, the single signal can only be explained either by a fixed D_{4d} or D_{4h} conformation or by a fast rotation of the rings in the NMR time scale. In the latter case, the conformation of the rings would have no influence at all on the

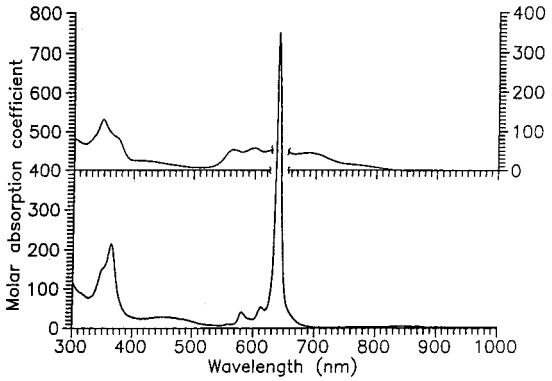

Figure 6. Extrapolated electronic absorption spectra of the two isomers of $[(H_{17}C_8O)_8PcSi(OSiMe_2tBu)_2]O$ (**10a**) present in benzene solution. Lower spectrum: D_{4h} or D_{4d} ("green") isomer. Upper spectrum: D_4 ("blue") isomer. Data for the D_4 isomer between 625 and 670 nm are of low accuracy because of the very steep absorption maximum of the other isomer in this range and are, therefore, omitted.

qualitative appearance of the spectrum. This idea was long ago introduced by Kenney but has never been experimentally verified.[48] To distinguish between these two possibilities, we performed low-temperature proton NMR measurements at −88 °C with compounds **10a**−**e** in dichloromethane-d_2 and toluene-d_6 (see Table 4). In dichloromethane, the signal of the aromatic protons $H^{b,b'}$ splits into two peaks of equal intensity at 7.9 and 8.9 ppm. The center of these two signals at 8.4 ppm corresponds well with the signal at 8.49 ppm found at room temperature in CD_2Cl_2. This demonstrates that the rotation of the rings in dichloromethane is free at room temperature but frozen at −88 °C, since we know from the UV/vis spectroscopic investigations that, in dichloromethane, only one isomer (the blue, less symmetrical one) is stable, irrespective of the temperature. Furthermore, this proves the μ-oxo-bridged dimers **10** to exist as the D_4 isomer in dichloromethane since we find two separate signals for H^b and $H^{b'}$. The strong splitting of $\Delta\delta = 1$ ppm between the two signals arises because proton H^b is situated more or less above the center of a benzene ring, whereas $H^{b'}$ is situated above the gap between two benzene rings of the underlying macrocycle (see Figure 1). Strong shift differences between the two protons are expected for torsion angles α between 20° and 30°, with a maximum at $\alpha = 25°$. The chemical shifts for H^b and $H^{b'}$ are not influenced at all by the nature of the peripheral alkoxy chains, neither at room temperature nor at −88 °C. The ring rotation α must be, therefore, the same for all five dimers, irrespective of the substituents. From the temperature dependence of the spectra, the barrier of rotation, $\Delta G^{\ddagger}$, was estimated to be 40.5 ± 0.4 kJ/mol at −54 °C for **10a**.

In toluene, the investigation of the optical spectra revealed that, at −88 °C, compounds **10a**−**e** exist as the pure or almost pure green, more symmetric, isomer. Accordingly, in the low-temperature ^{1}H-NMR spectra at −88 °C, only one singlet at 9.5 ppm for the aromatic protons was found, consistent with the assumption of exact or nearly exact D_{4h} or D_{4d} symmetry.[49] This has been already concluded from the UV/vis spectra.

The experimental results demonstrate the presence of one (nonaromatic solvents) or two (aromatic solvents) isomers of the dimers **10** in solution, differing in their torsional angle α.

In all nonaromatic solvents, only the D_4 isomer is stable, and the torsional angle α for this isomer is estimated from low-temperature ^{1}H-NMR measurements to be between 20° and 30°. This value is found to be also in good agreement with the UV/vis spectrum (see below). This demonstrates that the geometry adopted is an intrinsic property of the μ-oxo-bridged dimer and, in particular, not caused by any specific solvent−solute interaction (e.g., polar effects). Figure 7 shows a top view of a D_4 ($\alpha = 20°$), a D_{4d} ($\alpha = 45°$), and a D_{4h} ($\alpha = 0°$) isomer.[50] The separation of the peripheral substituents is maximized in the D_4 conformation ($\alpha = 20°$), causing it to be the most stable geometry. In the other two conformations, the alkyl chains are almost (D_{4d}) or exactly (D_{4h}) lying on top of each other. This results not only in a restricted spatial freedom of the chains but also in a quite close H^1(endo, ring 1)−H^1(endo, ring 2) distance of only about 1.9 Å in the D_{4d} conformation. Peripherally unsubstituted dimers show UV/vis spectra distinctly different from the spectrum for the alkoxy substituted D_4 isomer, and, hence, it is likely that their geometry is different. This demonstrates that the geometry of the dimers described in this paper is mainly controlled by the alkoxy substituents and not by the core. Since it is clear from the NMR data that the geometry of the D_4 isomer is not significantly influenced by the steric demand of the alkyl chain, the $C^{Ar}-O-C^1$ unit is responsible for the D_4 structure.

In aromatic solvents, a second isomer of $D_{4d/h}$ (or near $D_{4d/h}$) symmetry[51] is sufficiently stabilized to be in equilibrium with the D_4 isomer. The stabilization of the $D_{4d/h}$ isomer in aromatic solvents is likely to be due to specific solvent−solute interactions. We conclude this from the fact that the stabilization is a low-temperature phenomenon and specific for aromatic solvents. At higher temperatures, energetically favored but more ordered solvent−solute interactions become increasingly less important for entropic reasons.[52,53]

The $D_{4d/h}$ isomer is stable at low temperature, whereas the D_4 isomer becomes increasingly stabilized at higher temperatures. Attractive interactions between a substrate and aromatic solvents are not uncommon. They have been discussed, e.g., in the context of aromatic solvent-induced NMR shifts for a long time. Such interactions must be in operation in our case, since purely polar but nonaromatic solvents do not show any effect.

Linear alkoxy chains attached to the macrocycle cause a more stable $D_{4d/h}$ conformation (relative to D_4) than branched ones do. The 2-ethyl substituent in **10d** has a more destabilizing effect on the $D_{4d/h}$ conformation than the 3-methyl substituent in **10c**.

Neither for peripherally unsubstituted dimers[20] nor for oktaalkyl substituted dimers[54] is similar solvatochromic behavior

(48) Proton NMR spectra of the peripherally unsubstituted dimer were reported to be temperature independent in the temperature range between −20 and 150 °C.[30] However, this only excludes the possibility of a "frozen" D_4 conformation.

(49) Based on the observation of only one signal at −88 °C alone, D_{4h} or D_{4d} symmetry cannot be concluded. Strictly spoken, one signal could result as well from being above the coalescence temperature. However, if we assume being at or above coalescence and reasonably assume $\Delta G^{\ddagger}$ to be equal to or larger than that in CD_2Cl_2, the peak separation at slow exchange can be estimated to be less than 0.1 ppm. This is equivalent to exact or near D_{4d} or D_{4h} symmetry. It is very unlikely that the diminished peak separation is caused by distinctly different solvent-induced shifts, in particular because the situations in CD_2Cl_2 and in toluene-d_8 correspond to very different UV/vis spectra.

(50) The geometry of the macrocycle was taken from the following: Mooney, J. R.; Choy, C. K.; Knox, K.; Kenney, M. E. *J. Am. Chem. Soc.* **1975**, *97*, 3033−3038. The geometry of the peripheral alkoxy substituents was assumed as $C^{Ar}-OC^{Alk}$, 1.37 Å; $C^{Ar}O-C^{Alk}$, 1.43 Å; $C^{Ar}-O-C^{Alk}$, 118° (*Handbook of Chemistry and Physics*, 73rd ed.; Lide, D. R., Ed.; CRC Press: Boca Raton, 1992; pp 9-1−9-14. Nyburg, S. C.; Faermann, C. H. *J. Mol. Struct.* **1986**, *140*, 347−352).

(51) Here and in the following, $D_{4d/h}$ means D_{4d} or D_{4h} symmetry. In the present case, it is not possible to distinguish experimentally between these two geometries by qualitative arguments based on UV/vis or NMR spectra.

(52) (a) Price, S. L.; Stone, A. J. *J. Chem. Phys.* **1987**, *86*, 2859−2868. (b) Jorgensen, W. L.; Severance, D. L. *J. Am. Chem. Soc.* **1990**, *112*, 4768−4774.

(53) Hunter, C. A. *Chem. Soc. Rev.* **1994**, 101−109.

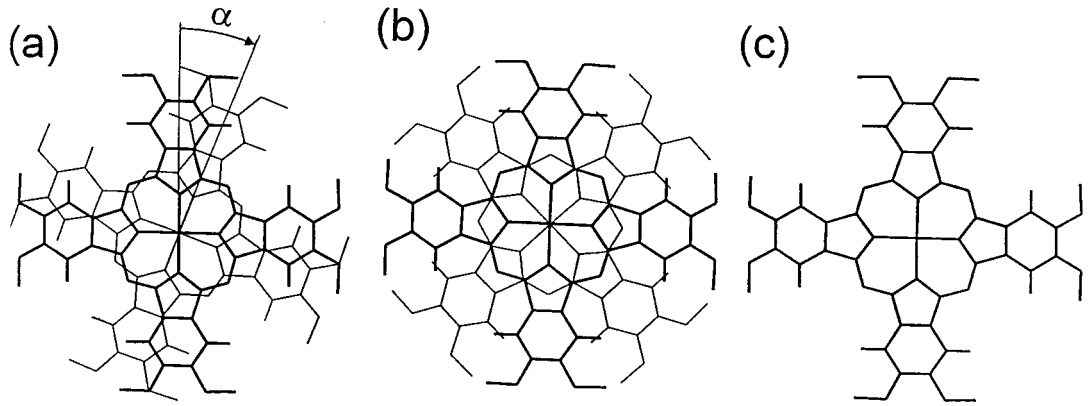

Figure 7. Top view of μ-oxo-bridged dimers $[(RO)_8PcSi(OSiMe_2tBu)]_2O$ (**10**) in different geometries. (a) $\alpha = 20°$ (D_4 symmetry), (b) $\alpha = 45°$ (D_{4d} symmetry), and (c) $\alpha = 0°$ (D_{4h} symmetry). For clarity, the axial siloxy ligands are omitted, and only the C^1 carbon atoms of the peripheral chains are shown.

Table 4. Proton NMR data for μ-Oxo-Bridged Dimers **10** (δ in ppm)[a]

	temp	H^{Si-Me}		H^{Si-tBu}		$H^{b,b'}$	
	(°C)	CD_2Cl_2	toluene	CD_2Cl_2	toluene	CD_2Cl_2	toluene
10a	−88	−4.19	−3.30	−2.41	−1.74	8.93/7.90	9.16
	+30	−4.07	−3.46	−2.29	−1.85	8.47	9.02
	+98		−3.53		−1.89		8.90
10c	−88	−4.20	−3.33	−2.41	−1.84	8.94/7.91	9.34
	+30	−4.06	−3.48	−2.28	−1.87	8.47	9.02
10d	−88	−4.20	−3.52	−2.41	−2.00	8.91/7.91	9.23
	+30	−4.00[b]	−3.54	−2.24[b]	−1.95	8.44[b]	8.96
10e	−88	−4.19	−3.30	−2.41	−1.76	8.94/7.90	9.17
		−4.25	−3.41		−1.89		
	+30	−4.06	−3.42	−2.28	−1.81	8.46	8.97
		−4.08	−3.53	−2.29	−1.93		

[a] Chemical shifts for the alkyl protons of the peripheral substituents are given in the experimental part. [b] In $CDCl_3$.

found. Support for the conclusion that attractive interactions between the aromatic hydrocarbon solvents and the macrocycle are responsible for the solvatochromism comes from the finding that no $D_{4d/h}$ isomer is observed for solutions in hexafluorobenzene due to the inverted electrostatic nature of this solvent. Since the D_4 geometry is mainly caused by the unique geometry of the alkoxy substituents, pronounced solvatochromism is neither expected nor found for unsubstituted μ-oxo-bridged dimers.

Considerable effort has been put into attempts to calculate and understand the electronic structure and the optical spectra of silicon phthalocyanine monomers and dimers.[14,20,26,28,29,55] However, so far, the comparison of experimental and theoretical spectra of dimers was complicated by three problems. First, there is a lack of reliable information about the torsion angle α in solution.[56] This angle is predicted to have a decisive influence on the electronic spectra. Second, the peripherally unsubstituted dimers investigated so far are thought to be a mixture of an unknown number of rotational isomers in solution. Third, complicated vibronic coupling between electronic states can affect the spectra severely, even in a simple model of exciton coupling.[57] In this work, we have obtained for the first time electronic absorption spectra of pure isomers of known symmetry. This allows for direct and reliable comparison of experimental and calculated data. The most detailed calculation with respect to the torsion angle is the one published by Ishikawa et al.[29] These results are in fairly good agreement with our experimental findings as shown below.[58]

Green Isomer, D_{4d} Symmetry, $\alpha = 45°$. In the relevant spectra, e.g., Figures 3 (solid line) and 6 (lower spectrum), we find a very intense transition at 639 nm, accompanied by a weak shoulder on its low-energy side and a very weak and broad transition around 830 nm.[59] The transitions at the high-energy side of the intense absorption at 639 nm are thought to be vibronic in origin, as they are in the monomers. The calculations predict[29] two allowed transitions. A strong one mainly to the allowed exciton-coupled state $2E_1$ at 643 nm corresponds well with our observed strong absorption at 639 nm. A weaker one is calculated at 697 nm and corresponds basically to the allowed component of the charge resonance transition ($1E_1$).

Blue Isomer, D_4 Symmetry, $\alpha \approx 20°$. The experimental data show five transitions at ~760, 703, 635, 598, and 561 nm (see Table 3 and Figures 2 and 6 (upper spectrum)). At $\alpha = 20°$, the calculated data are in good agreement with our experimental findings. Two bands of fairly high intensity are expected at 703 and 629 nm. The weak band at 760 nm can then be assigned to the lowest excited singlet state, which is forbidden under D_{4d} symmetry but gets some intensity under D_4 symmetry and should be found below 880 nm. The two transitions below 600 nm would then be vibronic in origin.

Concluding Remarks

This experimental work has shown that it is feasible to control the torsion angle α between adjacent macrocycles in μ-oxo-linked silicon phthalocyanines by the choice of peripheral substituents.[60] In octaalkoxy-substituted systems, the μ-oxo-bridged dimers $[(RO)_8PcSi(OR')]_2O$ (R = alkyl, R′ = e.g., silyl) are locked into a D_4 geometry, with α probably being close to 20°. This finding is important if the reasonable assumption is made that the same geometry is maintained in the corresponding polymers.[61,62] Calculations show that the bandwidth in poly-

(54) Kleinwächter, J. Ph.D. Thesis, University of Tübingen, Germany, 1994.

(55) Hale, P. D.; Pietro, W. J.; Ratner, M. A.; Ellis, D. E.; Marks, T. J. *J. Am. Chem. Soc.* **1987**, *109*, 5943−5947.

(56) The orientation in the solid state has been determined by X-ray analysis to be 36.6°,[20] but since the energetic barrier for ring ring rotation is very low, this value might be influenced significantly or even predominantly by packing effects in the solid state.

(57) Fulton, F. L.; Gouterman, M. *J. Chem. Phys.* **1964**, *41*, 2280−2286.

(58) The calculations were carried out for peripherally unsubstituted dimers, but the alkoxy substituents are not expected to influence the Q-band transitions significantly. However, higher excitations might be altered considerably by the interaction of the oxygen lone pairs with the phthalocyanine π-system.

(59) The second shoulder found in Figure 3 (see inset) around 690−700 nm is attributed to the presence of residual amounts of D_4 isomer.

(60) For the suggestion of this concept and for some of its consequences see ref. 13.

(61) For some evidence for a "close to"-eclipsed geometry in these polymers, see also: Kentgens, A. P. M.; Markies, B. A.; van der Pol, J. F.; Nolte, R. J. M. *J. Am. Chem. Soc.* **1990**, *112*, 8800−8806.

(62) Schouten, P. G.; Warman, J. M.; de Haas, M. P.; van der Pol., J. F.; Zwikker, J. W. *J. Am. Chem. Soc.* **1992**, *114*, 9028−9034.

(phthalocyaninato)siloxanes is determined by the torsion angle α and has a minimum for α = 19°, a value very close to the one we predict for the octaalkoxy-substituted polymers.

The concept of using peripheral substituents in order to control the torsion angle should be of general scope. The D_4 geometry observed for the systems described in this paper is a straightforward consequence of the C_{2v} geometry adopted by 1,2-bis(alkyloxy)benzenes. Use of different peripheral substituents should allow us to lock the rings into other geometries. If the oxygen would, e.g., be part of an annulated 1,4-dioxane ring system, one would expect a D_{4d} geometry for the dimers and polymers; the same is true if bulky substituents, e.g., *tert*-butyl, were used. Polymers of the latter system have been reported,[15] and the corresponding μ-oxo-bridged dimers have already been prepared.[54]

The finding that the μ-oxo-bridged dimers described in this paper can adopt two different geometries in aromatic solvents seems to be rather unique. It strongly suggests interactions between the solvent and the π-system of the aromatic solvent, and the compounds described might be a suitable system to study such interactions.

The detailed electronic absorption spectra of μ-oxo-linked silicon phthalocyanines in solution reported in this work for different (and well-defined) geometries allow for the first time, a verification of theoretical calculations, in particular with respect to the influence of the torsion angle α.

Experimental Section

Optical Spectroscopy. UV/vis spectra were recorded in quartz cells of 1 cm path length with a Perkin Elmer Lambda 5 spectrophotometer attached to a PC. Spectra at room temperature and above were taken in a thermostated sample cell. Low-temperature spectra were recorded in an Oxford Instruments variable-temperature liquid nitrogen cryostat DN1704 attached to a programmable temperature control unit. Solvents (benzene, toluene, and dichloromethane) were of spectrophotometric or HPLC grade and used as obtained. 1-Methylnaphthalene was of reagent grade (Aldrich, >98%) and passed through activated, basic alumina prior to use. Data points were taken in intervals of 0.5 nm at a scan speed of 30 nm/min and stored as ASCII data files to be processed later in a spreadsheet program as described in the text. Temperature-dependent Δ*G* values for the dimers **10** were calculated by a least-squares fit of a linear combination of the spectra of the pure isomers using all data points between 400 and 800 nm. The systematic error in Δ*G*, caused by the uncertainty in the determination of the spectra of the pure isomers, is <0.3 kJ/mol.

NMR spectra were recorded on Bruker WM400 and AC250 spectrometers. All signals were referenced to the residual solvent signal (CD_2Cl_2, 5.31 ppm (1H); $CDCl_3$, 7.25 ppm (1H), 77.0 ppm (^{13}C); C_6D_6, 7.15 ppm (^{1}H), 128.0 ppm (^{13}C); toluene-d_8, 7.09, 7.01, 6.97, 2.08 ppm (^{1}H)). In some cases, Gauss multiplication instead of exponential multiplication was applied to the FID in order to enhance the resolution. Low-temperature spectra were taken in 10 mm tubes, and the temperature was estimated from the temperature dependence of the ^{13}C chemical shifts in a neat sample of 2-chlorobutane (±4 °C).

IR spectra were recorded on a Bruker IFS 48 FT-IR spectrometer with a resolution of 4 cm^{-1}.

Solvents and Reagents. Quinoline was freshly distilled from calcium hydride under reduced pressure directly into the reaction vessel. Pyridine and $SiCl_4$ were distilled under nitrogen from calcium hydride, CH_2Cl_2 from P_4O_{10}, and THF from $LiAlH_4$/Ph_3CH. Tetrabutylammonium fluoride was dried for 48 h in vacuo prior to use (65 °C, 10^{-2} mbar). Precursors **1a**−**d** and **2a**−**d** were prepared according to methods reported in the literature.[17,63−65] All other chemicals were commercially available and used without further purification.

Syntheses. $(RO)_8PcSi(OH)_2$ (5a−d). These compounds were prepared by a modification of the method of van der Pol et al.[18] Quinoline (2 mL) was distilled under nitrogen into a Schlenk tube containing **2a**−**d** (5 mmol). The mixture was slowly heated up until a thick yellow solution was formed (∼60 °C). Silicon tetrachloride (1.6 mL, 2.4 g, 10 mmol) was added, and the mixture was quickly heated to 180 °C and kept at this temperature for the required reaction time (**2a** and **2b**, 20 h; **2c**, 6 h; **2d**, 3 h). After being cooled to room temperature, the reaction mixture was dissolved in $CHCl_3$ (30 mL). Pyridine (15 mL) and water (15 mL) were added, and the mixture was stirred at room temperature for 12 h. $CHCl_3$ (100 mL) was added, and the solid material was filtered off. After separating the phases, the organic phase was concentrated to about 20 mL and injected into rapidly stirred acetone. After the mixture was stirred for 18 h, the green precipitate was filtered off and purified twice by column chromatography on neutral alumina (400 g, activity IV, eluent first CH_2Cl_2, later CH_2Cl_2−diethyl ether (10%)), giving **5a**−**d** as green solids (**5a**, 55% (1.1 g); **5b**, 64% (1.65 g); **5c**, 59% (1.35 g); **5d**, 60% (1.2 g)).

For analytical data of **5a**,**b**, see refs 16 and 18. For UV spectra of **5a**−**d**, see Table 2.

5c. IR (KBr, cm^{-1}): 2955 s, 2926 s, 2868 m, 1607 m, 1520 m, 1501 m, 1466 s, 1425 s, 1391 s, 1364 m, 1283 s, 1205 m, 1115 m, 1086 s, 1009 w, 906 w, 822 m, 754 m, 739 m. Anal. Calcd for $C_{112}H_{178}N_8O_{10}Si$: C, 73.71; H, 9.83; N, 6.14. Found: C, 73.84; H, 10.35; N, 6.18.

5d. IR (KBr, cm^{-1}): 2959 s, 2928 s, 2874 m, 2860 m, 1607 m, 1520 m, 1501 m, 1479 s, 1462 vs, 1425 vs, 1389 m, 1362 m, 1281 s, 1205 m, 1115 m, 1086 s, 1059 m, 1020 m, 901 w, 858 vw, 845 w, 820 m, 754 m, 739 w. MS (FD, *m*/*z*): 1601.5 (calcd 1600.4). Anal. Calcd for $C_{96}H_{146}N_8O_{10}Si$: C, 72.05; H, 9.20; N, 7.00. Found: C, 71.74; H, 9.25; N, 6.79.

$(RO)_8PcSi(OSi(tBu)Me_2)_2$ (6a−d). 5a−d (300 μmol) was dissolved in dry CH_2Cl_2 (200 mL) and dry pyridine (3 mL). At 0 °C, *tert*-butyldimethylsilyl trifluormethanesulfonate (3 mmol, 683 μL) was added [or, alternatively, *tert*-butyldimethylsilanol (6 mmol) and trifluoromethanesulfonic acid (150 μL, 1.7 mmol)]. The reaction was kept for 2 h at 0 °C and 12 h at room temperature before it was poured into water (200 mL, 0 °C). The organic phase was separated, washed with $NaHCO_3$ solution and water, and evaporated to dryness. The residue was purified by column chromatography on neutral alumina (activity IV, toluene as eluent). The green microcrystalline product obtained by this procedure (yield 95−100%) was normally free of μ-oxo-bridged dimer. However, if *tert*-butyldimethylsilyl trifluoromethanesulfonate was added at room temperature, sometimes traces of μ-oxo-bridged dimer were formed. They can be separated by column chromatography on alumina (activity IV) using *n*-hexane−toluene (55/45) as eluent. The μ-oxo-bridged dimers elute slightly faster than the monomer.

For UV spectra of **6a**−**d**, see Table 2.

6a. IR (KBr, cm^{-1}): 2926 m, 2854 m, 1607 m, 1522 w, 1502 m, 1481 m, 1464 s, 1427 s, 1391 m, 1360 m, 1283 s, 1246 w, 1205 m, 1097 s, 1057 s, 1005 w, 914 w, 891 w, 858 w, 831 m, 810 w, 770 w, 758 m, 743 w, 723 w, 694 w, 673 w, 630 w. MS (FD, *m*/*z*): 1829.4 (calcd 1828.9). ^{1}H NMR ($CDCl_3$, 250 MHz): δ 9.05 (s, 8H, H^b), 4.69 (t, *J* = 6.5 Hz, 16H, H^1), 2.19 (m, 16H, H^2), 1.77 (m, 16H, H^3), 1.75−130 (m, 64H, H$^{4-7}$), 0.95 (t, *J* = 6.8 Hz, 24H, H^8), −1.43 (s, 18H, $C(CH_3)_3$), −2.99 (s, 12H, $Si(CH_3)_2$). ^{1}H NMR (C_6D_6, 250 MHz): δ 9.48 (s, 8H, H^b), 4.14 (t, *J* = 6.3 Hz, 16H, H^1), 1.88 (m, 16H, H^2), 1.56 (m, br, 16H, H^3), 1.35 (br, 64H, H$^{4-7}$), 0.97 (m, 24H, H^8), −0.97 (s, 18H, $C(CH_3)_3$), −2.32 (s, 12H, $Si(CH_3)_2$). ^{13}C NMR (C_6D_6, 62.5 MHz): δ 152.6 (C^a), 149.3 (C^d), 130.7 (C^c), 106.3 (C^b), 69.5 (C^1), 32.2 (C^6), 29.8 (3 signals, C^{2,4,5}), 26.6 (C^3) 24.0 ($C(CH_3)_3$), 23.1 (C^7), 15.9 ($C(CH_3)_3$), 14.4 (C^8), −6.4 ($Si(CH_3)_2$). Anal. Calcd for $C_{108}H_{174}N_8O_{10}Si_3$: C, 70.92; H, 9.59; N, 6.13. Found: C, 71.21; H, 10.00; N, 6.09.

6b. IR (KBr, cm^{-1}): 2953 sh, 2924 vs, 2854 s, 1607 w, 1522 w, 1502 m, 1481 m, 1464 s, 1427 s, 1391 s, 1358 m, 1281 s, 1246 w, 1205 m, 1097 s, 1057 s, 1005 w, 897 w, 831 w, 771 w, 758 m, 743 w. MS (FD, *m*/*z*): 2279.5 (calcd 2277.8). ^{1}H NMR (CDCl3): δ 9.05 (s, 8H, H^b), 4.68 (t, *J* = 6.3 Hz, 16H, H^1), 2.18 (m, 16H, H^2), 177 (m, 16H, H^3), 16.2−1.18 (m, 128H, H$^{4-11}$), 0.89 (t, *J* = 6.6 Hz, 24H, H^{12}), −1.43 (s, 18H, $C(CH_3)_3$), −2.98 (s, 12H, $Si(CH_3)_2$). ^{1}H NMR (C_6D_6, 250 MHz): δ 9.48 (s, 8H, H^b), 4.15 (t, *J* = 6.1 Hz, 16H, H^1), 1.90 (m,

(63) Lelievre, D.; Bosio, L.; Simon, J.; Andre, J.-J.; Bensebaa, F. *J. Am. Chem. Soc.* **1992**, *114*, 4475−4479.

(64) van der Pol, J. F.; Neeleman, E.; Zwicker, J. W.; Nolte, R. J. M.; Drenth, W. *Recl. Trav. chim. Pays-Bas* **1988**, *107*, 615−620.

(65) Schouten, P. G.; van der Pol, J. F.; Zwicker, J. W.; Drenth, W.; Picken, S. J. *Mol. Cryst. Liq. Cryst.* **1991**, *195*, 291−305.

16H, H^2), 1.59 (m, br, 16H, H^3), 1.46−1.28 (m, br, 128H, H^{4-11}), 0.94 (m, 24H, H^{12}), −0.97 (s, 18H, $C(CH_3)_3$), −2.32 (s, 12H, $Si(CH_3)_2$). ^{13}C NMR ($CDCl_3$, 62.5 MHz): δ 152.7 (C^a), 148.2 (C^d), 129.8 (C^c), 105.8 (C^b), 69.8 (C^1), 32.0 (C^{10}), 29.8/29.7/29.6/29.4 ($C^{2,4-9}$), 26.4 (C^3), 23.4 ($C(CH_3)_3$), 22.7 (C^{11}), 15.2 ($C(CH_3)_3$), 14.7 (C^{12}), −7.2 ($Si(CH_3)_2$). ^{13}C NMR (C_6D_6, 62.5 MHz): δ 153.6 (C^a), 149.3 (C^d), 130.7 (C^c), 106.2 (C^b), 69.6 (C^1), 32.4 (C^{10}), 30.2 (3 signals)/29.9 (3 signals) ($C^{2,4-9}$), 26.7 (C^3), 24.4 ($C(CH_3)_3$), 23.1 (C^{11}), 15.9 ($C(CH_3)_3$), 14.4 (C^{12}), −6.4 ($Si(CH_3)_2$). Anal. Calcd for $C_{140}H_{238}N_8O_{10}Si_3$: C, 73.83; H, 10.53; N, 4.92. Found: C, 74.24; H, 10.86; N, 4.86.

6c. IR (KBr, cm^{-1}): 2953 s, 2928 s, 2870 m, 1607 m, 1522 m, 1502 m, 1481 m, 1466 s, 1427 s, 1391 s, 1360 m, 1283 s, 1246 m, 1205 m, 1097 s, 1057 s, 1005 m**,** 978 w, 906 m, 858 w, 831 w, 770 w, 758 m, 743 w. ^1H NMR (C_6D_6, 250 MHz): δ 9.49 (s, 8H, H^b), 4.22 (t, J = 6.2 Hz, 16H, H^1), 2.10−1.15 (nm, 80H, H^{2-7}), 1.04 (d, J = 6.3 Hz, 24H, H^{10}), 0.97 (2d, J = 6.6 Hz, 48H, $H^{8,9}$), −0.99 (s, 18H, $C(CH_3)_3$), −2.33 (s, 12H, $Si(CH_3)_2$). ^{13}C NMR (C_6D_6, 62.5 MHz): δ 153.6 (C^a), 149.3 (C^d), 130.6 (C^c), 106.1 (C^b), 67.9 (C^1), 39.7/37.9/36.9 ($C^{2,4,6}$), 30.4/28.4 (C,^{3,7}), 25.3 (C^5), 24.0 ($C(CH_3)_3$), 23.0/22.9 ($C^{8,9}$), 20.0 (C^{10}), 15.9 ($C(CH_3)_3$), −6.4 ($Si(CH_3)_2$). Anal. Calcd for $C_{124}H_{206}N_8O_{10}Si_3$: C, 72.54; H, 10.11; N, 5.46. Found: C, 72.74; H, 10.43; N, 5.36.

6d. IR (KBr, cm^{-1}): 2957 s, 2928 s, 2874 m, 2858 m, 1607 w, 1522 w, 1503 m, 1481 s, 1462 s, 1427 vs, 1389 m, 1360 m, 1283 s, 1246 w, 1205 m, 1097 vs, 1057 s, 1005 w, 927 w, 899 w, 858 w, 831 w, 770 w, 758 m, 744 w. MS (FD, *m*/*z*): 1829.5 (calcd 1828.9). ^1H NMR ($CDCl_3$, 250 MHz): δ 9.04 (s, 8H, H^b), 4.58 (m, 16H, H^1), 2.11 (m, 8H, H^2), 1.76 (m, 32H, $H^{3,7}$), 1.57 (br), 149 (2 m, 32H, $H^{4,5}$), 1.15 (t, J = 7.5 Hz, 24H, H^8), 1.01 (m, 24H, H^6), −1.44 (s, 18H, $C(CH_3)_3$), −2.99 (s, 12H, $Si(CH_3)_2$). ^1H NMR (C_6D_6, 250 MHz): δ 9.50 (s, 8H, H^b), 4.9 (br, 16H, H^1), 1.9−1.3 (nm, 72H, $H^{2-5,7}$), 1.03 (t, J = 7.3 Hz, 24H, H^8), 1.01 (t, J = 7.1 Hz, 24H, H^6), −1.00 (s, 18H, $C(CH_3)_3$), −2.33 (s, 12H, $Si(CH_3)_2$). ^{13}C NMR ($CDCl_3$, 250 MHz): δ 152.9 (C^a), 148.2 (C^d), 129.7 (C^c), 105.4 (C^b), 72.1 (C^1), 40.0 (C^2), 31.0/29.4 ($C^{3,4}$), 24.3/23.5/23.2 ($C^{5,7}$, $C(CH_3)_3$), 15.3 ($C(CH_3)_3$), 14.2 (C^6), 11.5 (C^8), −7.2 ($Si(CH_3)_2$). Anal. Calcd for $C_{108}H_{174}N_8O_{10}Si_3$: C, 70.93; H, 9.59; N, 6.13. Found: C, 71.04; H, 9.90; N, 5.94.

$(RO)_8PcSi(F)(OSi(tBu)Me_2)$ (7a,d). Tetrabutylammonium fluoride (150 mg) and trifluoroacetic acid (1.5 mL) were added to a solution of **6a,d** in dry THF (100 mL). The solution was stirred at room temperature until all starting material had reacted (about 36 h, checked by TLC, SiO_2, *n*-hexane−CH_2Cl_2−diethyl ether (45/45/10)). The reaction mixture was then poured into water (300 mL) and extracted with CH_2Cl_2. The organic phase was washed with $NaHCO_3$ solution and water and evaporated to dryness. The residue was purified by column chromatography (SiO_2, traces of starting material may be eluted with CH_2Cl_2−*n*-hexane (50/50), while with CH_2Cl_2 (for **7b**) or CH_2Cl_2−Et_2O (1.3%) (for **7a**), the product was isolated. Yield: 95%, green powder.

For UV spectra of **7a,d**, see Table 2.

7a. IR (KBr, cm^{-1}): 2955 m, 2926 s, 2853 m, 1605 w, 1522 w, 1502 m, 1481 m, 1466 s, 1427 s, 1391 s, 1362 m, 1281 s, 1261 w, 1248 w, 1238 w, 1207 m, 1096 s, 1057 m, 1045 m, 997 w, 986 w, 912 w, 899 w, 889 w, 878 w, 862 w, 831 w, 818 w, 762 m, 744 w, 735 w, 721 w. MS (FD, *m*/*z*): 1716.7 (M^+, calcd 1716.6), 3433.6 ($2M^+$, calcd 3433.2), 3414.8 ({2M − HF}$^+$ = μ-fluoro-bridged dimer$^+$, calcd 3414.2). ^1H NMR ($CDCl_3$, 250 MHz): δ 9.03 (s, 8H, H^b), 4.67 (t, J = 6.5 Hz, 16H, H^1), 2.18 (m, 16H, H^2), 1.77 (m, 16H, H^3), 1.60−1.25 (nm, 64H, H^{4-7}), 0.94 (m, 24H, H^8), −1.41 (s, 18H, $C(CH_3)_3$), −2.95 (s, 12H, $Si(CH_3)_2$). ^1H NMR (C_6D_6, 250 MHz): δ 8.88 (br, 8H, H^8), 3.79 (br, 16H, H^8), 1.86, 1.81 (2 m, 16H, $H^{2,2'}$), 1.36 (nm, 80H, H^{3-7}), 1.01 (t, J = 6.7 Hz, 24H, H^8), −1.25 (s, 9H, $C(CH_3)_3$), −2.60 (s, 6H, $Si(CH_3)_2$). ^{13}C NMR ($CDCl_3$, 62.5 MHz): δ 152.9 (C^a), 148.6 (C^d), 129.7 (C^c), 105.7 (C^b), 69.9 (C^1), 31.9 (C^6), 29.6/29.4 ($C^{2,4,5}$), 26.3 (C^3), 23.4 ($C(CH_3)_3$), 22.7 (C^7), 15.2 ($C(CH_3)_3$), 14.1 (C^8), −7.3 ($Si(CH_3)_2$). Anal. Calcd for $C_{102}H_{159}N_8FO_9Si_2$: C, 71.36; H, 9.34; N, 6.53; F, 1.11. Found: C, 71.35; H, 9.53; N, 6.10; F, 1.45.

7d. IR (KBr, cm^{-1}): 2957 s, 2928 s, 2872 m, 2858 m, 1607 m, 1524 m, 1502 m, 1481 s, 1462 s, 1427 s, 1389 s, 1362 m, 1281 s, 1246 m, 1207 m, 1097 s, 1059 s, 1043 m, 930 w, 901 m, 856 w, 845 w, 831 w, 762 m, 744 w, 667 w. MS (FD, *m*/*z*): 1716.4 (M^+, calcd 1716.6), 3432.9 ($2M^+$, calcd 3433.2), 3414.3 ({2M − HF}$^+$ = μ-fluoro-bridged dimer$^+$, calcd 3414.2). ^1H NMR ($CDCl_3$): δ 9.06 (s, 8H, H^b), 4.60 (m, 16H, H^1), 2.15 (m, 8H, H^2), 1.80, 1.55 (nm, 2 × 32H, $H^{3-5,7}$), 1.18 (2t, J = 7.4 Hz, 24H, H^8), 1.04 (2t, J = 6.4 Hz, 24H, H^6), −1.37 (s, 9H, $C(CH_3)_3$), −2.91 (s, 6H, $Si(CH_3)_2$). ^{13}C NMR ($CDCl_3$): δ 153.2 (C^a), 148.7 (C^d), 129.7 (C^c), 105.3 (C^b), 72.2 (C^1), 39.9 (C^2), 31.0/29.4 ($C^{3,4}$), 24.3/23.2 ($C^{5,7}$), 23.4 ($C(CH_3)_3$), 15.2 ($C(CH_3)_3$), 14.2 (C^8), −7.1 ($Si(CH_3)_2$). Anal. Calcd for $C_{102}H_{159}N_8FO_9Si_2$: C, 71.36; H, 9.34; N, 6.53; F, 1.11. Found: C, 72.57; H 10.02; N, 6.45; F, 1.38.

$(RO)_8PcSi(OH)(OSi(tBu)Me_2)$ (8a,d). **7a,d** (360 μmol) was dissolved in dry CH_2Cl_2 (100 mL) and dry pyridine (3 mL). Trimethylsilyl triflate (Me_3SiOTf; 650 μL, 800 mg, 3.6 mmol) was added, and the brown-yellow mixture was stirred for 2 h at room temperature. The reaction mixture was poured into water (400 mL), and the organic phase was separated and washed with water, $NaHCO_3$ solution, and again with water. After evaporation to dryness, the crude product was subjected to column chromatography (SiO_2). CH_2Cl_2 eluted the byproduct **9a,d** as a green microcrystalline powder. Yield: **9a**, 35% (226 mg, 126 μmol); **9d**, 34% (218 mg, 122 μmol). **8a,d** was then eluted with CH_2Cl_2−Et_2O (10%), to give a green microcrystalline powder. Yield: **8a**, 61% (376 mg, 220 μmol); **8d**, 58% (360 mg, 210 μmol).

For UV spectra of **8a,d** and **9a,d**, see Table 2.

8a. IR (KBr, cm^{-1}): 2924 s, 2853 m, 1605 m, 1518 m, 1501 m, 1466 s, 1425 s, 1389 s, 1362 m, 1281 s, 1246 m, 1205 m, 1090 s, 1059 m, 1038 m, 1005 m, 918 w, 893 m, 858 w, 831 w, 766 m, 760 m, 743 w, 725 w. MS (FD, *m*/*z*): 1714.6 (M^+, calcd 1714.6), 3410.8 ({2M − H_2O}$^+$ = μ-oxo-bridged dimer$^+$, calcd 3411.2), 3429.0 ($2M^+$, calcd 3429.2). ^1H NMR ($CDCl_3$): δ 8.7 (s, br, 8H, H^b), 4.5 (br, 16H, H^1), 2.11 (br, 16H, H^2), 1.70 (br, 16H, H^3), 1.65−1.30 (br, 64H, H^{4-7}), 0.95 (t, J = 6.7 Hz, 24H, H^8), −1.61 (s, br, 9H, $C(CH_3)_3$), −3.19 (s, br, 6H, $Si(CH_3)_2$). ^1H NMR (C_6D_6): δ 9.55, 9.13, 6.74 (3 s, br, 8H, H^b), 4.47, 4.20, 2.75 (3 s, br, 16H, H^1), 1.98 (br, 16H, H^2), 1.63 (br, 16H, H^3), 1.41 (64H, H^{4-7}), 1.02 (t, J = 6.4 Hz, 24H, H^8), −1.36 (s, br, 9H, $C(CH_3)_3$), 0.34, −2.66 (s, 1H, OH, monomeric and aggr. (?)), −2.75 (s, br, 6H, $Si(CH_3)_2$). ^{13}C NMR ($CDCl_3$, 62.5 MHz): δ 152.5 (C^a), 148.0 (C^d), 129.3 (C^c), 105.7 (C^b), 69.8 (C^1), 32.0 (C^6), 29.7/29.6/29.5 ($C^{2,4,5}$), 26.3 (C^3), 23.1 ($C(CH_3)_3$), 22.8 (C^7), 14.9 ($C(CH_3)_3$), 14.2 (C^8), −7.6 ($Si(CH_3)_2$). Anal. Calcd for $C_{102}H_{160}N_8O_{10}Si_2$: C, 71.45; H, 9.41; N, 6.54. Found: C, 71.13; H, 9.95, N, 6.53.

8d. IR (KBr, cm^{-1}): 2959 s, 2872 s, 2858 s, 1607 m, 1520 m, 1501 m, 1481 s, 1462 s, 1425 s, 1387 s, 1362 m, 1283 s, 1246 m, 1205 m, 1105 s, 1092 s, 1059 m, 1036 m, 899 m, 858 w, 829 w, 760 m, 744 w. MS (FD, *m*/*z*): 1705.3 ({2M − H_2O}$^{2+}$ = μ-oxo-bridged dimer^{2+}, calcd 1705.6), 1714.8 (M^+, calcd 1714.6), 3411.1 ({2M − H_2O}$^+$ = μ-oxo-bridged dimer$^+$, calcd 3411.2), 3429.0 ($2M^+$, calcd 3429.2). ^1H NMR ($CDCl_3$, 250 MHz): δ 9.02 (s, 8H, H^b), 4.57 (s, br, 16H, H^1), 2.11 (m, 8H, H^2), 1.76, 1.49 (nm, 64H, $H^{3-5,7}$), 1.15 (2t, J = 7.4 Hz, 24H, H^8), 1.01 (2t, J = 7.2 Hz, 24H, H^6), −1.45 (s, 9H, $C(CH_3)_3$), −3.00 (s, 6H, $Si(CH_3)_2$). ^1H NMR (C_6D_6): δ 9.49, 9.20, 6.81 (3s, br, 8H, H^b), 4.31, 4.16, 2.76 (3s, br, 16H, H^1), 1.77, 1.48 (br, 72H, $H^{2-5,7}$), 1.07 (br, 48H, $H^{6,8}$), −1.43 (br, 9H, $C(CH_3)_3$), −2.72 (s, OH (?)), −2.83 (br, 6H, $Si(CH_3)_2$). ^{13}C NMR ($CDCl_3$, 62.5 MHz): δ 153.0 (C^a), 148.3 (C^d), 129.7 (C^c), 105.3 (C^b), 72.1 (C^1), 39.9 (C^2), 30.9/29.4 ($C^{3,4}$), 24.2, 23.2 ($C^{5,7}$), 23.4 ($C(CH_3)_3$), 15.2 ($C(CH_3)_3$), 14.2 (C^6), 11.5 (C^8), −7.3 ($Si(CH_3)_2$). Anal. Calcd for $C_{102}H_{160}N_8O_{10}Si_2$: C, 71.45; H, 9.41; N, 6.54. Found: C, 71.20; H, 9.70; N, 6.41.

$[(RO)_8PcSi(OSi(tBu)Me_2))_2O$ (10a−d). Dimethyl-*tert*-butylsilyl triflate (27 μL, 32 mg, 120 μmol) in dry CH_2Cl_2 (4 mL) was added dropwise to a solution of **5a**−**d** (120 μmol) in dry CH_2Cl_2 (60 mL) and dry pyridine (200 mL) at −78 °C. Stirring was continued for 6 h at −78 °C before the solution was slowly warmed over a period of 12 h and left at room temperature for the required reaction time (**10a** and **10b**, 6 h; **10c**, 12 h; **10d**, 7 days (!)). The reaction can be followed by UV spectroscopy in CH_2Cl_2. The reaction mixture was poured into water, and the organic phase was immediately separated and washed with water, $NaHCO_3$ solution, and again with water. The solvent was evaporated, and the redissolved residue (*n*-hexane/10% CH_2Cl_2 (2 mL)) was subjected to column chromatography (neutral alumina, activity IV). With toluene, a mixture of **6a**−**d** and **10a**−**d** was eluted. A mixture of hydroxy substituted compounds could be eluted with CH_2Cl_2−Et_2O (5%). **6a**−**d** and **10a**−**d** were separated by PTLC on neutral alumina (Merck) using toluene−*n*-hexane mixtures as eluent (**10a** (40/60), **10b** (35/65), **10c** (30/70), **10d** (20/80)). After extraction with CH_2Cl_2 from the plates, the blue dimers were obtained as slightly sticky solids.

Yield: **10a**, 28% (17 μmol, 57 mg); **10b**, 7.8% (4.7 μmol, 20 mg); **10c**, 24% (14 μmol, 55 mg); **10d**, 29% (17 μmol, 59 mg).

For UV spectra of **10a**−**d**, see Table 3.

10a. IR (KBr, cm^{-1}): 2953 s, 2924 s, 2854 m, 1609 m, 1520 m, 1501 m, 1481 m, 1466 s, 1429 s, 1391 s, 1360 m, 1285 s, 1261 w, 1244 w, 1236 w, 1204 w, 1096 s, 1059 m, 1036 m, 1005 w, 997 w, 988 w, 914 w, 891 w, 852 w, 831 w, 770 w, 754 m. MS (FD, *m*/*z*): 3412.8 (M^+, calcd 3411.2), 1706.4 (M^{2+}, calcd 1705.6). ^{1}H NMR ($CDCl_3$, 50 MHz): δ 8.45 (s, 16H, $H^{b,b'}$), 4.82/4.61 (2m, 32H, H^1), 2.33 (m, 32H, H^2), 1.92 (m, 32H, H^3), 1.69 (m, 32H, H^4), 1.59 (m, 32H, H^5), 1.48 (m, 64H, $H^{6,7}$), 1.01 (m, 48H, H^8), −2.27 (s, 18H, $C(CH_3)_3$), −4.03 (s, 12H, $Si(CH_3)_2$). ^{1}H NMR (C_6D_6, 400 MHz): δ 9.11 (s, 16H, $H^{b,b'}$), 4.51/4.05 (2m, 32H, H^1), 2.19/2.10 (2m, 32H, H^2), 1.74 (m, br, 32H, H^3), 1.54/1.46 (2m, br, 128H, H^{4-7}), 1.03 (t, J = 6.3 Hz, 48H, H^8), −1.84 (s, 18H, $C(CH_3)_3$), −3.40 (s, 12H, $Si(CH_3)_2$). ^{13}C NMR (C_6D_6, 100 MHz): δ 152.8 (C^a), 147.8 (C^d), 130.2 (C^c), 106.7 (C^b), 69.8 (C^1), 32.4 (C^6), 30.5, 30.3, 30.0 ($C^{2,4,5}$), 26.9 (C^3), 23.3 ($C(CH_3)_3$), 23.2 (C^7), 15.0 ($C(CH_3)_3$), 14.4 (C^8), −7.4 ($Si(CH_3)_2$). Anal. Calcd for $C_{204}H_{318}N_{16}O_{109}Si_4$: C, 71.82; H, 9.40; N, 6.57. Found: C, 72.44; H, 9.93; N, 6.43.

10b. IR (KBr, cm^{-1}): 2955 s, 2926 s, 2870 m, 1609 m, 1522 w, 1501 m, 1481 m, 1466 s, 1427 s, 1391 s, 1360 m, 1285 s, 1246 w, 1236 w, 1204 m, 1171 w, 1097 s, 1059 m, 1038 m, 986 w, 906 w, 854 w, 829 w, 806 w, 754 m. ^{1}H NMR (C_6D_6, 400 MHz): δ 9.13 (s, 16H, $H^{b,b'}$), 4.54/4.08 (2m, 32H, H^1), 2.22/2.14 (2m, 32H, H^2), 1.80 (m, br, 32H, H^3), 1.7−1.3 (nm, br, 256H, H^{4-11}), 0.98 (t, J = 6.7 Hz, 48H, H^{12}), −1.82 (s, 18H, $C(CH_3)_3$), −3.38 (s, 12H, $Si(CH_3)_2$). ^{13}C NMR (C_6D_6, 100 MHz): δ 152.8 (C^a), 147.8 (C^d), 130.1 (C^c), 106.6 (C^b), 69.8 (C^1), 32.4 (C^{10}), 30.59, 30.52, 30.48, 30.44, 30.44, 30.33 ($C^{2,4-9}$), 27.0 (C^3), 23.3 ($C(CH_3)_3$), 23.2 (C^{11}), 15.0 ($C(CH_3)_3$), 14.4 (C^{12}), −7.4 ($Si(CH_3)_2$).

10c. IR (KBr, cm^{-1}): 2922 s, 2853 s, 1609 w, 1520 w, 1501 m, 1481 m, 1466 s, 1427 m, 1391 m, 1360 m, 1285 m, 1246 w, 1234 w, 1204 m, 1094 m, 1061 m, 1036 m, 1005 w, 986 w, 918 w, 895 w, 852 w, 831 w, 810 w, 754 m, 723 w. ^{1}H NMR (CD_2Cl_2, 250 MHz): δ 8.51 (vbr, 16H, $H^{b,b'}$), 4.90/4.69 (2m, br, 32H, H^1), 2.49 (br, 8H), 2.37 (br, 8H), 2.19 (br, 24H), 2.08 (br, 8H), 1.8−1.4 (br, 96H), 1.4−1.3 (br, 40H), 1.28 (d, 24H), 1.08−0.91 (nd, 96H), −2.25 (s, 18H, $C(CH_3)_3$), −4.04 (s, 12H, $Si(CH_3)_2$). ^{1}H NMR (C_6D_6, 250 MHz): δ 9.08 (s, br, 16H, $H^{b,b'}$), 4.73/4.20 (2m, br, 32H, H^1), 2.46 (br, 8H), 2.23 (br, 8H), 2.09 (br, 24H), 1.89 (br, 8H), 1.8−1.2 (nm, br, 136H), 1.21 (d, J = 6.2 Hz, 24H, H^{10}), 1.07 (2d, J = 6.6 Hz, 48H, $H^{8,9}$), 1.025 (d, J = 6.5 Hz, 24H, $H^{8,9}$), 1.015 (d, J = 6.5 Hz, 24H, $H^{8,9}$), −1.84 (s, 18H, $C(CH_3)_3$), −3.39 (s, 12H, $Si(CH_3)_2$). ^{13}C NMR (C_6D_6, 100 MHz): δ 152.8/152.7 (C^a), 147.5 (C^d), 130.1 (C^c), 106.2 (C^b), 68.2/67.9 (C^1), 39.95/39.93/39.87/39.85 (C^6), 38.76/38.68, 38.23/38.17 ($C^{2,4}$), 30.80/30.48/30.44 (C^3), 28.52/28.49 (C^7), 25.58/25.56/25.51 (C^5), 23.3 ($C(CH_3)_3$), 23.08/23.03, 22.98/22.92 ($C^{8,9}$), 20.63/20.56/19.96 (C^{10}), 15.0 ($C(CH_3)_3$, −7.4 ($Si(CH_3)_2$). Anal. Calcd for $C_{204}H_{318}N_{16}O_{109}Si_4$: C, 73.43; H, 9.97; N, 5.81. Found: C, 74.42; H, 10.56; N, 5.64.

10d. IR (KBr, cm^{-1}): 2959 s, 2928 s, 2874 m, 2858 m, 1609 m, 1522 w, 1501 m, 1479 s, 1464 s, 1427 s, 1387 m, 1360 m, 1285 s, 1248 w, 1202 m, 1096 s, 1059 m, 1036 m, 986 w, 924 w, 899 m, 878 w, 852 w, 841 w, 829 w, 770 w, 754 m, 735 w. MS (FD, *m*/*z*): 3411.1 (M^+, calcd 3411.2), 3280.4 (M − $OSiMe_2tBu)^+$, calcd 3279.9). ^{1}H NMR ($CDCl_3$, 250 MHz): δ 8.44 (br, 16H, $H^{b,b'}$), 4.48/4.32 (2br, 32H, H^1), 2.22 (br, 16H, H^2), 2.00−1.40 (nm, br, 128H, $H^{3-5,7}$), 1.27 (t, J = 7.1 Hz, 48H, H^6), 1.05 (t, J = 6.6 Hz, 48H, H^8), −2.24 (s, 18H $C(CH_3)_3$), −4.00 (s, 12H, $Si(CH_3)_2$). ^{1}H NMR (C_6D_6, 250 MHz): δ 9.03 (s, 16H, $H^{b,b'}$), 4.64/4.05 (2br, 32H, H^1), 2.22 (br, 16H, H^2), 2.1−1.5 (nm, br, 128H, $H^{3-5,7}$), 1.32/1.27 (2t, J = 7.3 Hz, 48H, H^6), 1.13/1.11 (2t, J = 7.0 Hz, 48H, H^8), −1.90 (s, 18H, $C(CH_3)_3$), −3.46 (s, 12H, $Si(CH_3)_2$). ^{13}C NMR (C_6D_6, 100 MHz): δ 153.0 (C^a), 147.3 (C^d), 130.0/129.9 (C^c), 106.0/105.9 (C^b), 72.64/72.21 (C^1), 40.41/40.44 (C^2), 30.98/30.34/30.10/29.61 ($C^{3,4}$), 2429/24.22/23.80/23.76 ($C^{5,7}$), 23.3/23.2 ($C(CH_3)_3$), 14.9 ($C(CH_3)_3$), 14.55/14.22 (C^6), 12.24/11.58 (C^8), −7.3 ($Si(CH_3)_2$). Anal. Calcd for $C_{204}H_{318}N_{16}O_{109}Si_4$: C, 71.82; H, 9.40; N, 6.57. Found: C, 72.20; H, 9.86; N, 6.07.

[($H_{17}C_8O$)$_8$PcSi(OSi(tBu)Me_2)]$_2$O (10a), from 8a. Trifluoromethanesulfonic acid (9 mg, 5 μL, 57 μmol) was added to a solution of **8a** (80 mg, 47 μmol) and dry pyridine (1 mL) in dry CH_2Cl_2 (15 mL). The reaction was stirred at room temperature for 12 h and worked up described as above. Yield: **10a**, 38% (30 mg, 9 μmol).

[(2-Et-$C_6H_{12}O$)$_8$PcSi(OSi(tBu)Me_2)]$_2$O (10d), from 5d. Trifluoromethanesulfonic acid (17 mg, 10 μL, 114 μmol) was added to a solution of **5d** (160 mg, 100 μmol) and dry pyridine (2 mL) in dry CH_2Cl_2 (20 mL). The reaction was stirred at room temperature for **7d**. Dimethyl-*tert*-butylsilyl triflate (348 mg, 300 μL, 1.32 mmol) was added, and stirring was continued for a further 24 h before **10d** was isolated as described above. Yield: **10d**, 60% (103 mg, 30 μmol).

($H_{17}C_8O$)$_8$PcSi(OSiMe_2tBu)O(2-Et-$C_6H_{12}O$)$_8$PcSi(OSiMe_2tBu) (10e). To a solution of **8a** (32 mg, 19 mmol) and **5d** (30 mg, 19 mmol) in dry CH_2Cl_2 (10 mL) were added dry pyridine (35 μL) and trifluoromethanesulfonic acid (3 mg, 2 μL, 23 μmol) at room temperature. After the mixture was stirred for 4 h, pyridine (1 mL) and dimethyl-*tert*-butylsilyl triflate (116 mg, 100 μL, 439 μmol) were added, and stirring was continued for 24 h. The reaction can be followed by UV spectroscopy in CH_2Cl_2. The reaction mixture was poured into water (100 mL), and the organic phase was immediately separated and washed with water, $NaHCO_3$ solution, and again with water. The solvent was evaporated, and the residue (dissolved in *n*-hexane−10% CH_2Cl_2 (2 mL) was subjected to column chromatography (neutral alumina, activity IV). With toluene, a mixture of **6a**, **6d**, **10a**, **10d**, and **10e** was eluted. A mixture of hydroxy-substituted compounds could be eluted with CH_2Cl_2−Et_2O (5%). Separation of compounds **6** and **10** was achieved by TLC for **6d** and **10e** (in that order), while **10a** and **6a** did not move. They could be separated in a second step using toluene−*n*-hexane (40/60) as eluent. After extraction from the PTLC plates with CH_2Cl_2, the blue dimers were obtained as slightly sticky solids. Yield: **10e**, 30% (5.6 μmol, 19 mg).

10e. UV: see Table 3. IR (KBr, cm^{-1}) 2957 s, 2926 s, 2856 m, 1609 m, 1522 m, 1501 m, 1481 s, 1462 s, 1427 s, 1389 s, 1358 m, 1285 s, 1246 w, 1204 m, 1096 s, 1059 m, 1038 m, 988 w, 899 w, 852 w, 829 w, 754 m. ^{1}H NMR (CD_2Cl_2, 250 MHz): δ 8.46 (br, 16H, $H^{b,b'}${C_8, 2-Et-C_6}), 4.84/4.76/4.61/4.49 (4m, br, 32H, H^1 {C_8, 2-Et-C_6}), 2.3 (m, 24H, H^2 {C_8, 2-Et-C_6}), 1.9 (m, 48H)1.8−1.5 (m, 64H)/1.43 (m, 32H ($H^{3-5,7}$ {2-Et-C_6}, H^{3-7} {C_8}), 1.32 (2t, J = 7.3 Hz, 24H, H^8 {2-Et-C_6}), 1.09 (t, J = 7.0 Hz, 24H, H^6 {2-Et-C_6}), 0.99 (m, 24H, H^8 {C_8}), −2.28/−2.29 (2s, 18H, $C(CH_3)_3$), −4.08 (2s, 12H, $Si(CH_3)_2$). ^{1}H NMR (C_6D_6, 400 MHz): δ 9.04 (s, 16H, $H^{b,b'}$ {C_8, 2-Et-C_6}), 4.63/4.52/4.13/4.04 (4m, 32H, H^1 {C_8, 2-Et-C_6}), 2.29 (m, 8H, H^2 {2-Et-C_6}), 2.15 (m, 16H, H^2 {C_8}), 2.1−1.7 (m, 48H)/1.6 (2m, 64H)/1.5 (m, 32H, $H^{3-5,7}$ {2-Et-C_6}, H^{3-7} {C_8}), 1.31 (2t, 24H, H^8 {2-Et-C_6}), 1.15 (t, J = 6.5 Hz, 24H, H^6 {2-Et-C_6}), 103 (t, 6.7 Hz, 24H, H^8 {C_8}), −1.80/−1.89 (2s, 18H, $C(CH_3)_3$), −3.36/−3.44 (2s, 12H, $Si(CH_3)_2$). ^{13}C NMR (C_6D_6): δ 152.8/152.7 (C^a), 147.43/147.42 (C^d), 106.0/105.8 (br, C^b), 129.9 (C^c), 72.29/71.92 (C^1 {2-Et-C_6}), 69.55 (C^1 {C_8}), 40.69/40.86/40.84 (C^2 {2-Et-C_6}), 32.42 (C^6 {C_8}), 31.48/31.14/30.13/29.86 ($C^{3,4}$ {2-Et-C_6}), 30.55/30.30/30.02 ($C^{2,4,5}$ {C_8}), 26.96 (C^3 {C_8}), 24.46/24.43/24.35/24.32/23.83/23.79/23.30/23.24 ($C^{5,7}$ {f2-Et-C_6}), C^7 {C_8}, $C(CH_3)_3$), 15.0/14.9 ($C(CH_3)_3$ 14.59/14.57 (C^6 {2-Et-C_6}), 14.42 (C^8 {C_8}), 12.26/11.83 (C^8 {2-Et-C_6}), −7.3/−7.4 ($Si(CH_3)_2$).

Acknowledgment. We thank the Fonds der Chemischen Industrie for the financial support of this work. We thank Dr. O. Ohno, Department of Materials Science, Faculty of Engineering, Ibaraki University, Hitachi, Japan, for his kind help with the assignment of the electronic transition of the dimers. We are indebted to Dr. T. Bjornholm, CISMI, University of Copenhagen, Denmark, for supporting us with the equipment for the low-temperature UV/vis measurements and for his kind hospitality and assistance during the stay of J.K. in Copenhagen. We also thank Dr. L. R. Subramanian for his help in preparing the manuscript.

Supporting Information Available: ^{1}H NMR spectra of **8a** and **10a**−**e** and UV/vis spectra of **10a** (various temperatures), **10b**,**c** (various temperatures), and **10e** (53 pages). See any current masthead page for ordering and Internet access instructions.

JA962663F